Mannose impairs tumour growth and enhances chemotherapy

Pablo Sierra Gonzalez[1], James O'Prey[1], Simone Cardaci[1,4], Valentin J.A. Barthet[1], Jun-ichi Sakamaki[1], Florian Beaumatin[1], Antonia Roseweir[2], David Gay[1], Gillian Mackay[1], Gaurav Malviya[1], Elżbieta Kania[1], Shona Ritchie[1], Alice D. Baudot[1], Barbara Zunino[1], Agata Mrowinska[1], Colin Nixon[1], Darren Ennis[2], Aoisha Hoyle[3], David Millan[3], Iain A. McNeish[2], Owen J. Sansom[1,2], Joanne Edwards[2] and Kevin M. Ryan[1,2*]

[1]Cancer Research UK Beatson Institute,
Garscube Estate, Switchback Rd,
Glasgow, G61 1BD, UK

[2]Institute of Cancer Sciences,
University of Glasgow,
Garscube Estate, Switchback Road,
Glasgow G61 1QH, UK

[3]Department of Pathology,
Queen Elizabeth University Hospital,
Glasgow, G51 4TR, UK

[4]Division of Genetics and Cell Biology
San Raffaele Scientific Institute,
Via Olgettina, 58, 20132 Milano - ITALY

Running title: Role for mannose in cancer therapy.

∗Correspondence:

Kevin Ryan
Cancer Research UK Beatson Institute
Tel: +441413303655
E-mail: k.ryan@beatson.gla.ac.uk

Introductory paragraph

It is now well established that tumours undergo changes in cellular metabolism[1]. As this can reveal tumour cell vulnerabilities and because many tumours exhibit enhanced glucose uptake[2], we have been interested in how tumour cells respond to different forms of sugar. Here we report that the monosaccharide mannose causes growth retardation in multiple tumour types and enhances cell death in response to major forms of chemotherapy. Importantly, we go on to show that these effects also occur following oral administration of mannose *in vivo* without significant impact on animal weight and health. Mechanistically, mannose is taken up by the same transporter(s) as glucose[3], but accumulates as mannose-6-phosphate in cells and this impairs the further metabolism of glucose in glycolysis, the TCA cycle, the pentose phosphate pathway and glycan synthesis. As a result, when used in combination with conventional chemotherapy, this has an impact on protein levels of anti-apoptotic members of the Bcl-2 family leading to sensitization to cell death. Finally, we show that susceptibility to mannose is dependent on the levels of phosphomannose isomerase (PMI). Cells with low levels of PMI are sensitive to mannose, whereas cells with high levels are resistant, but can be made sensitive by RNAi-mediated depletion of the enzyme. In addition, we show using tissue microarrays that PMI levels also vary greatly between different patients and different tumour types, indicating that PMI levels could be used as a biomarker to direct successful mannose administration. When taken together, we consider that treatment with mannose could be a simple, safe and selective way to treat cancer applicable to multiple tumour types.

As tumours often have a high avidity for glucose[4], we examined the impact of other sugars on tumour cell growth. This revealed that mannose, in contrast to other sugars, significantly reduced U2OS cell growth (Fig. 1a). Similar effects occurred in Saos-2 cells, with fucose also causing a comparatively small decrease in cell growth (Extended Data Fig. 1a). Using a panel of cell lines, we observed that this effect of mannose occurs in cells from various tissues, with the impact being greater in some cells than others (Fig. 1b,c, Extended Data Fig. 1a-d).

Mannose is imported into cells via the same transporters as glucose[3], so we considered mannose may interfere with glucose uptake. Supporting this hypothesis, we observed that mannose enhances phospho-AMPK levels – a readout of energy balance in cells[5,6] (Extended Data Fig. 1e). However, liquid chromatography-mass spectrometry (LC-MS) showed that levels of the phosphorylated form of the glucose analogue 2-deoxyglucose (2-DG-P), used as a proxy for glucose uptake, did not correlate with mannose sensitivity in mannose-sensitive versus insensitive lines (Figure 1a,b; Extended Data Fig. 1f,g), and mannose actually increased the intracellular pool of hexose-6-phosphate (the first step in metabolism of glucose and mannose) (Extended Data Fig. h). This effect was not observed with other sugars (Extended Data Fig.1i).

To determine if the mannose-induced increase in hexose-6-phosphate is due to mannose or glucose, we performed LC-MS with an extended chromatography time to enable selective detection of the unphosphorylated form of these sugars. This revealed that mannose increased the intracellular pool of mannose, as expected, but also increased the intracellular pool of glucose (Extended Data Fig. 1j, k). To corroborate, we treated cells with glucose labelled with two atoms of ^{13}C (1,2-$^{13}C_2$-Glucose) and mannose labelled with six atoms of

^{13}C ($^{13}C_6$-Mannose) to enable detection due to differences in molecular mass and we again found that mannose treatment increased intracellular glucose levels (Extended Data Fig. 1l).

As mannose did not reduce intracellular glucose, but significantly impacted cell growth, we considered it may interfere with glucose metabolism. There is considerable crosstalk between the metabolism of these sugars and mannose-6-phosphate can inhibit three enzymes that mediate glucose metabolism: hexokinases, phosphoglucose isomerase (PGI) and glucose-6-phosphate dehydrogenase (G6PDH)[7] (Fig. 1d). To address this possibility, we measured the levels of hexose-6P and lactate when cells were incubated in glucose-free medium supplemented with either 1,2-$^{13}C_2$-Glucose or $^{13}C_6$-Mannose. This revealed that mannose accounts for more of the mannose-induced hexose-6P accumulation than glucose, but also that glucose-6P is produced in the presence of mannose, albeit at reduced levels when compared with cells treated with glucose alone (Fig. 1e). We also observed that mannose does not produce much lactate (indicating it is poorly metabolised) and more importantly, that mannose markedly reduces lactate production from glucose (Fig. 1f). Further analysis revealed that mannose treatment not only affects pools of glycolytic intermediates, but also those involved in the TCA cycle, pentose phosphate pathway and glycan synthesis (Fig. 1g-i). As with the effects on cell growth, these metabolic effects were not observed with other sugars (Extended Data Fig. 1m-p). Moreover, while mannose uptake was not lower in mannose-insensitive cells when compared to sensitive cells (Extended Data Fig. 2a), the effects of mannose on metabolism were only observed in cells sensitive to the sugar (Extended Data Fig. 2b-h). Interestingly, we also found that mannose-induced AMPK phosphorylation does not concomitantly occur with changes in the levels of AMP or ATP, but is associated with a decrease in Fructose-1,6-bisphosphate levels as recently described[6] (Extended Data 3a-f).

Because mannose affects tumour cell growth, we questioned whether it can also affect the cellular response to chemotherapeutic drugs. While mannose alone did not affect cell viability, it significantly enhanced cell death when administered with cisplatin or doxorubicin - an effect not seen with other hexoses (Figs 2a,b; Extended Data Fig. 4a-c). Mechanistically, the combination of mannose and chemotherapeutic drug increased the levels of cleaved PARP (a substrate of caspase-3[8]) and this effect, together with death, was blocked by the pan-caspase inhibitor zVAD-fmk (Fig. 2c,d; Extended Data Fig. 4d).

As our data indicated that cell death from mannose and chemotherapeutic drug likely proceeds by apoptosis, we utilised CRISPR/Cas9 to determine which apoptotic pathways might be involved. Disruption of caspase 8 and FADD – two components of the extrinsic apoptotic pathway[9] –had no impact on the cell death observed (Extended Data Fig. 4e-g). In contrast, disruption of Bax and Bak - essential factors for mitochondrial outer membrane permeabilisation (MOMP) and the intrinsic pathway[10] – significantly blocked death from mannose in combination with either cisplatin or doxorubicin (Fig. 2e; Extended Data Fig. 4h,i).

MOMP is controlled by Bcl-2 family members,[11] so we examined the levels of these proteins in the presence of mannose, cisplatin or in combination. In line with previous studies detailing a role for the Noxa/Mcl-1 axis in glycolysis inhibition and glucose deprivation,[12-14] we found Noxa was increased by cisplatin and cisplatin plus mannose, and Mcl-1 and Bcl-X_L were reduced by the combination treatment (Fig. 2f; Extended Data Fig. 4j). Mechanistically, we consider Mcl-1 and Bcl-X_L are diminished through decreased translation as they decreased in the presence of proteasome inhibitor and their mRNAs were not reduced

by the combination treatment (Extended Data Fig 2k-m). Involvement of these proteins was confirmed by CRISPR-mediated disruption of *noxa* or by over-expression of Mcl-1 or Bcl-$X_{L,}$ which all repressed death induced by mannose and chemotherapy (Fig. 2g,h; Extended Data Fig. 4n-q; Extended Data 5a). Finally, we also observed that mannose enhances death induced by the Bcl-X_L antagonist WEHI539, but not the Bcl-2 antagonist ABT-199 (Extended Data Figure 5b).

We were keen to know if mannose also has effects *in vivo*. Tumour-bearing mice were therefore given a single oral gavage of mannose, which resulted in a serum concentration of approximately 3mM (Extended Data Fig. 6a). Animals were then injected with 2-deoxy-2-(^{18}F)fluoro-D-glucose (^{18}F-FDG) to monitor ^{18}F-FDG uptake and its subsequent conversion by hexokinases into ^{18}F-FDG-6-P[15]. As mannose impedes hexokinases[6], we found it significantly reduced the ^{18}F-FDG signal (provided by ^{18}F-FDG and/or ^{18}F-FDG-6-P) when tumours of equivalent size in each condition were compared (Fig. 3a; Extended Data Fig. 6b,c). A significant effect on the ^{18}F-FDG signal was also seen in certain normal tissues (Extended Data Fig. 6d).

To test if mannose could affect tumour growth, animals were injected with tumour cells subcutaneously and given mannose by oral gavage 3 times per week and *ad libitum* in drinking water. This did not affect animal weight, nor did it visibly affect animal health, (Extended Data Fig. 6e), but it significantly inhibited tumour growth (Fig. 3b), involving decreased numbers of BrdU-positive cells, indicating that mannose inhibits cell proliferation both *in vitro* and *in vivo* (Extended Data Fig. 6f,g).

We were also interested to know if mannose can also enhance chemotherapy *in vivo*. Tumour-bearing nude mice were therefore treated with mannose and doxorubicin either alone or in combination. While none of the treatments affected the weight or visible health of the animals (Extended Data Fig. 6h), we found that either doxorubicin or mannose caused a reduction in tumour volume (Fig. 3c). Moreover, when doxorubicin was administered in combination with mannose an even greater effect was observed (Fig. 3c). Importantly, when we examined the overall survival of the treated cohorts, those treated with doxorubicin plus mannose had a significantly increased life expectancy when compared to untreated mice or those treated with either doxorubicin or mannose alone (Fig. 3d).

As our data indicated that mannose could potentially be used clinically, we wanted to understand why different cells vary in their sensitivity to the sugar. Because mannose affects several metabolic pathways, we reasoned that sensitivity may be connected to an apical enzyme involved in sugar metabolism. Our profiling revealed that mannose sensitivity was roughly inversely correlated with the levels and activity of phosphomannose isomerase (PMI) - the enzyme that catalyses the interconversion of mannose-6P and fructose-6P[16] (Fig 4a; Extended Data Fig. 7a; Fig. 1a-c; Extended Data Figure 1 b-d,f). Consequently, we knocked-down PMI in 3 mannose-insensitive cell lines – SKOV3, RKO and IGROV1. In each case, PMI knockdown caused growth retardation upon mannose treatment (Fig. 4b; Extended Data Fig. 7b-g) and dramatically sensitized cells to cell death when mannose was administered together with cisplatin (Fig. 4c). Conversely, PMI over-expression in a mannose-sensitive line rendered the line refractory to the effects of mannose on both cell growth and cell death (Fig. 4d; Extended Data Fig. 7h-k). Finally, we found that mannose treatment following PMI knockdown had highly significant effects on metabolic pathways downstream of the sugar (Fig 4e; Extended Data Fig. 7l-o).

We next questioned if PMI could be modulated to affect the response of tumours to mannose *in vivo*. Since the immune microenvironment is important in many therapeutic situations and because mannose can affect immune cell function[17,18], we decided to utilize immune-competent mice and two syngeneic cell lines (B16-F1 and LLC) which are ordinarily mannose-insensitive, but which become sensitive upon PMI knockdown (Fig. 4f,g; Extended Data Fig. 8a-d). In both cases, allografts formed with PMI knockdown cells were highly sensitive to oral administration of mannose (Fig. 4h-k), without visibly affecting animal health or weight (Extended Data Fig. 8e-h)

We were also interested to know if PMI levels varied in human tumours such that analysis of PMI could potentially be used as a biomarker for mannose sensitivity. We therefore stained tissue microarrays (TMAs) containing sections from ovarian, renal, breast, prostate and colorectal cancers. This revealed that PMI levels varied between tumours from the same tissue and also between tissues (Fig. 4l; Extended Data Fig. 9a). PMI levels did not, however, have prognostic significance in breast and colon cancer, presumably because normal serum levels of mannose are low compared to glucose[19](Extended Data Fig. 9b-d).

Most notable from our analyses was the fact that colorectal tumours generally have very low PMI levels, indicating they may be broadly sensitive to mannose. To explore this, we utilised an inflammation-driven model of colorectal cancer and a genetically engineered mouse model (GEMM) driven by two genes frequently altered in this disease (K-Ras and APC)[20]. In both models, mice maintained on drinking water containing 20% mannose had significantly fewer tumours at endpoint (Fig. 4m,n) and importantly, mannose had no

negative impact on the health or weight of the animals over the time examined (Extended Data Fig. 9e,f).

In contrast to the effects on glucose metabolism, mannose does not decrease amino acid or fatty acid uptake and while mannose reduces glucose-dependent serine and glycine synthesis, this contributes only marginally to total cellular serine and glycine pools (Extended Data Fig. 10a-f). Mannose also affects transcription, translation and autophagy, but these effects were reversed by PMI over-expression, indicating they are downstream of glucose metabolism (Extended Data Fig. 10g-l). Moreover, ablation of autophagy did not affect mannose sensitivity showing that autophagy inhibition is not the mechanism underlying the effects of the sugar (Extended Data Fig. 10m,n). In summary, we conclude that mannose represents a well-tolerated means to interfere with glucose metabolism that could potentially be used clinically either alone or in combination with other forms of cancer therapy.

References

1 Hanahan, D. & Weinberg, R. A. Hallmarks of cancer: the next generation. *Cell* **144**, 646-674, doi:10.1016/j.cell.2011.02.013 (2011).

2 Pavlova, N. N. & Thompson, C. B. The Emerging Hallmarks of Cancer Metabolism. *Cell metabolism* **23**, 27-47, doi:10.1016/j.cmet.2015.12.006 (2016).

3 Thorens, B. & Mueckler, M. Glucose transporters in the 21st Century. *American journal of physiology. Endocrinology and metabolism* **298**, E141-145, doi:10.1152/ajpendo.00712.2009 (2010).

4 Cairns, R. A., Harris, I. S. & Mak, T. W. Regulation of cancer cell metabolism. *Nature reviews. Cancer* **11**, 85-95, doi:10.1038/nrc2981 (2011).

5 Chaube, B. & Bhat, M. K. AMPK, a key regulator of metabolic/energy homeostasis and mitochondrial biogenesis in cancer cells. *Cell death & disease* **7**, e2044, doi:10.1038/cddis.2015.404 (2016).

6 Zhang, C. S. *et al.* Fructose-1,6-bisphosphate and aldolase mediate glucose sensing by AMPK. *Nature* **548**, 112-116, doi:10.1038/nature23275 (2017).

7 DeRossi, C. *et al.* Ablation of mouse phosphomannose isomerase (Mpi) causes mannose 6-phosphate accumulation, toxicity, and embryonic lethality. *The Journal of biological chemistry* **281**, 5916-5927, doi:10.1074/jbc.M511982200 (2006).

8 Fischer, U., Janicke, R. U. & Schulze-Osthoff, K. Many cuts to ruin: a comprehensive update of caspase substrates. *Cell death and differentiation* **10**, 76-100, doi:10.1038/sj.cdd.4401160 (2003).

9 Elmore, S. Apoptosis: a review of programmed cell death. *Toxicologic pathology* **35**, 495-516, doi:10.1080/01926230701320337 (2007).

10 Westphal, D., Dewson, G., Czabotar, P. E. & Kluck, R. M. Molecular biology of Bax and Bak activation and action. *Biochimica et biophysica acta* **1813**, 521-531, doi:10.1016/j.bbamcr.2010.12.019 (2011).

11 Tait, S. W. & Green, D. R. Mitochondria and cell death: outer membrane permeabilization and beyond. *Nature reviews. Molecular cell biology* **11**, 621-632, doi:10.1038/nrm2952 (2010).

12 Pradelli, L. A. *et al.* Glycolysis inhibition sensitizes tumor cells to death receptors-induced apoptosis by AMP kinase activation leading to Mcl-1 block in translation. *Oncogene* **29**, 1641-1652, doi:10.1038/onc.2009.448 (2010).

13 Alves, N. L. *et al.* The Noxa/Mcl-1 axis regulates susceptibility to apoptosis under glucose limitation in dividing T cells. *Immunity* **24**, 703-716, doi:10.1016/j.immuni.2006.03.018 (2006).

14 Coloff, J. L. *et al.* Akt-dependent glucose metabolism promotes Mcl-1 synthesis to maintain cell survival and resistance to Bcl-2 inhibition. *Cancer research* **71**, 5204-5213, doi:10.1158/0008-5472.CAN-10-4531 (2011).

15 Quirce, R. *et al.* New insight of functional molecular imaging into the atheroma biology: 18F-NaF and 18F-FDG in symptomatic and asymptomatic carotid plaques after recent CVA. Preliminary results. *Clinical physiology and functional imaging* **36**, 499-503, doi:10.1111/cpf.12254 (2016).

16 Sharma, V., Ichikawa, M. & Freeze, H. H. Mannose metabolism: more than meets the eye. *Biochemical and biophysical research communications* **453**, 220-228, doi:10.1016/j.bbrc.2014.06.021 (2014).

17 Chattopadhyay, U. & Bhattacharyya, S. Inhibition by monosaccharides of tumor associated macrophages mediated antibody dependent cell cytotoxicity to autologous tumor cells. *Neoplasma* **34**, 295-303 (1987).
18 Gartner, S. L. & Williams, T. J. Modulation of interleukin-1 induced thymocyte proliferation by D-mannose. *Thymus* **19**, 117-126 (1992).
19 Alton, G. *et al.* Direct utilization of mannose for mammalian glycoprotein biosynthesis. *Glycobiology* **8**, 285-295 (1998).
20 De Robertis, M. *et al.* The AOM/DSS murine model for the study of colon carcinogenesis: From pathways to diagnosis and therapy studies. *Journal of carcinogenesis* **10**, 9, doi:10.4103/1477-3163.78279 (2011).

References in Online Methods

21 Long, J. S. *et al.* Extracellular adenosine sensing-a metabolic cell death priming mechanism downstream of p53. *Molecular cell* **50**, 394-406, doi:10.1016/j.molcel.2013.03.016 (2013).
22 Riley, J. S. *et al.* Mitochondrial inner membrane permeabilisation enables mtDNA release during apoptosis. *The EMBO journal*, doi:10.15252/embj.201899238 (2018).
23 Sanjana, N. E., Shalem, O. & Zhang, F. Improved vectors and genome-wide libraries for CRISPR screening. *Nature methods* **11**, 783-784, doi:10.1038/nmeth.3047 (2014).
24 Sakamaki, J. I. *et al.* Bromodomain Protein BRD4 Is a Transcriptional Repressor of Autophagy and Lysosomal Function. *Molecular cell* **66**, 517-532 e519, doi:10.1016/j.molcel.2017.04.027 (2017).
25 Mrschtik, M. *et al.* DRAM-3 modulates autophagy and promotes cell survival in the absence of glucose. *Cell death and differentiation* **22**, 1714-1726, doi:10.1038/cdd.2015.26 (2015).
26 Meiser, J. *et al.* Serine one-carbon catabolism with formate overflow. *Science advances* **2**, e1601273, doi:10.1126/sciadv.1601273 (2016).
27 Karvela, M. *et al.* ATG7 regulates energy metabolism, differentiation and survival of Philadelphia-chromosome-positive cells. *Autophagy* **12**, 936-948, doi:10.1080/15548627.2016.1162359 (2016).
28 Rosenfeldt, M. T. *et al.* E2F1 drives chemotherapeutic drug resistance via ABCG2. *Oncogene*, doi:10.1038/onc.2013.470 (2013).
29 Rosenfeldt, M. T. *et al.* p53 status determines the role of autophagy in pancreatic tumour development. *Nature* **504**, 296-300, doi:10.1038/nature12865 (2013).
30 Cammareri, P. *et al.* TGFbeta pathway limits dedifferentiation following WNT and MAPK pathway activation to suppress intestinal tumourigenesis. *Cell death and differentiation* **24**, 1681-1693, doi:10.1038/cdd.2017.92 (2017).

Acknowledgements

We thank John Knight, David Lewis, and Emma Johnson for help and advice. This work was supported by Worldwide Cancer Research (16-1194) and Cancer Research UK (A15816 and A17196).

Author Contributions

KMR, PSG and ADB conceived the study. PSG, JOP, JS, FB, EK, SR conducted and anaysed cell growth, cell death and enzyme assays and western blotting. PSG, SC, GMacK conducted and analysed metabolic experiments. VB, DG, BZ performed animal experiments. GM and AM performed and analyzed PET-MRI. CN performed immunohistochemistry. AR, DE, AH, and DM generated and analysed TMAs . PSG and KMR wrote the manuscript. IMcN, OJS, JE and KMR supervised the study. SC and VB contributed equally to this study.

Conflict of Interest Statement

The authors declare no competing interests.

Corresponding author information:

Kevin Ryan
Cancer Research UK Beatson Institute
Glasgow G61 1BD, UK
Tel: +441413303655
FAX: +441419426521
E-mail: k.ryan@beatson.gla.ac.uk

Figure Legends

Figure 1: Mannose impairs cancer cell growth and interferes with glucose metabolism by accumulating as mannose-6-phosphate intracellularly. (a) Growth curves of U2OS cells supplemented without (Ctrl) or with 25mM of hexoses (Man, mannose; Gal, galactose; Fru, fructose; Fuc, fucose; Glc, glucose). (b-c) Growth curves of (b) Saos-2 cells in DMEM (-Man) or with additional 25mM mannose (+Man) and (c) KP-4 cells in IMDM medium with or without 25mM mannose. (d) Scheme of mannose metabolism: mannose enters the cells using the same (GLUT) transporters as glucose and it is phosphorylated into mannose-6-phosphate by hexokinases (HK). Mannose can then be used for glycosylation purposes or isomerized into fructose-6-phosphate by phosphomannose isomerase (PMI). Glucose-6-phosphate can also produce mannose-6-phosphate by phosphoglucose isomerase (PGI) and PMI. Mannose-6-phosphate also participates in the biosynthesis of deaminoeuraminic acid (KDN). (e,f) Extraction of intracellular metabolites and measurement of the peak area per microgram of protein of (e) glucose-6-phosphate (m+2) and mannose-6-phosphate (m+6) and (f) lactate (m+0, m+2, m+3) after 6 hours incubation of U2OS cells in 10% dialyzed FBS glucose-free DMEM complete medium in the presence of 5mM 1,2-$^{13}C_2$-D-glucose alone and or 5mM $^{13}C_6$-D-mannose. (g-i) Percentage of peak area per microgram of protein of intracellular metabolites (g) glyceraldehyde-3-phosphate (GA3-P) and phosphoenolpyruvate (PEP); (h) α-ketoglutarate (α-KG) and malate; (i) ribose-5-phosphate (Ribose-5P) and UDP-N-Acetyl-glucosamine (UDP-GlcNAc) post 6-hours incubation of U2OS cells in 10% dialyzed FBS 5mM glucose DMEM complete medium with or without 5mM mannose. n=3 independent experiments (a,b,c,g,h,i). Data are representative of three independent experiments (e,f). Data are mean +/- S.E.M.. Data were analysed by (a-c) two-way ANOVA

with Bonferroni correction or (g-i) paired two-tailed Student's t-test. *P < 0.05, **P < 0.01, ***P < 0.001.

Figure 2: Combination of chemotherapy with mannose enhances cell death by potentiating the intrinsic pathway of apoptosis through the downregulation of Mcl-1 and Bcl-X_L protein levels. (a-h) All experiments were performed by pre-incubating cells in the presence of complete DMEM or 25mM sugars-supplemented complete DMEM for 24 hours prior to addition of other treatments. (a-b) Percentage of U2OS-E1a and Saos-2 propidium iodide (PI)-positive cells after 24 h treatment with (a) 10μM cisplatin and (b) 1μg/mL of doxorubicin in the presence or absence of 25mM mannose. (c) Percentage of U2OS-E1a PI-positive cells treated for 24 hours with or without 10μM cisplatin, with or without 25mM mannose and with or without 10μM of the caspase inhibitor zVAD-fmk. (d) Western blotting showing the levels of cleaved PARP and cleaved caspase-3 in U2OS-E1a cells after 24 hours treatment with or without 10μM cisplatin, with or without 25mM mannose and with or without 50μM zVAD-fmk. (e) Percentage of Empty and Bax/Bak CRISPR U2OS-E1a PI-positive cells treated with or without 10μM cisplatin for and with or without 25mM mannose for 24 h. (f) Western blotting showing the levels of Mcl-1, Bcl-X_L and cleaved caspase-3 in U2OS-E1a cells after 24h with or without 10μM cisplatin, with or without 25mM mannose and with or without 50μM zVAD-fmk. (g,h) Percentage of PI-positive U2OS-E1a (Emtpy, Mcl-1 and Bcl-X_L overexpressing) cells after 24 h treatment with or without 10μM cisplatin and with or without 25mM mannose. n=3 independent experiments (a,b,c,e,g,h). Data are representative of three independent experiments (d,f). Data are mean +/- S.E.M.. Data were analysed by (a,b,c,e,g,h) two-way ANOVA with Bonferroni correction. *P < 0.05, **P < 0.01, ***P < 0.001.

Figure 3: Mannose impairs tumour growth and induces tumour regression in combination with chemotherapy. (a) CD1-nude mice were transplanted with KP-4 cells subcutaneously and tumours were grown for 14 days before PET-MRI imaging. (a) PET-MRI scan of mice treated with 200µL of water (-Man) or 20% (w/v) mannose in water (+Man) by oral gavage 20 min before ^{18}F-FDG tail vein injection. White dotted circles highlight tumour areas in axial view of the mice. (b) CD1-nuce mice were injected with KP-4 cells subcutaneously and treated with normal drinking water (-Man) or 20% mannose in the drinking water (w/v) plus the same treatment via oral gavage 3 days per week from the 3rd day after tumour transplantation. Tumour volume (mm^3) was measured as indicated. (c,d) CD1-nude mice were injected with KP-4 cells subcutaneously and tumours were grown for 10 days before mannose treatment started. Mice received normal drinking water (Ctrl and Doxo) or 20% mannose in the drinking water (Man and Doxo + Man) together with the same treatment via oral gavage 3 days per week. Doxorubicin treatment started on day 32 and mice received 5mg/kg by IP injection once per week. (c) Tumour volume (mm^3) of all groups of treatment. (d) Graph representing the survival of the animals in all groups of treatment until the end of the experiment at day 73. Mice number for each experiment is (a) n=5, -Man; n=4, +Man, (b) n=10, -Man; n=8, +Man (c,d) n=10/group. Data are mean +/- S.E.M.. Data were analyzed by two-way ANOVA with Bonferroni correction (b,c) or log-rank (two-sided Mantel-Cox) (d). **P < 0.01, ***P < 0.001.

Figure 4: PMI levels dictate mannose sensitivity. (a) Western blot showing the levels of PMI and ERK2 in a panel of 10 cancer cell lines. (b) Growth curves of SKOV3 cells in complete DMEM medium with or without supplementation of 25mM mannose after transient

transfection with 2 non-targeting (NTC) and 2 PMI targeting siRNAs individially for 48 hours. (c) Cell death represented as percentage of PI-positive SKOV3 siRNA transfected cells pre-incubated with or without 25mM mannose in regular DMEM for 24 hours before adding 10μM of cisplatin for another 24 h. (d) Over-expression of PMI makes U2OS insensitive to mannose. Growth curves of U2OS overespressing PMI (U2OS-PMI) and cells expressing vectrol control (U2OS) after culture in either in DMEM (black line) or DMEM containing 25mM mannose (blue line). (e) Percetange of hexoses-6P metabolic content in SKOV3 transfected cells with siRNA for 48 h before 6 h incubation in complete DMEM medium with or without supplementation of 25mM mannose. (f,g) Knockdown of PMI renders B16-F1 and LLC cells sensitive to mannose. The indicated cell were incubated with or without 25mM mannose for 24h before cell counting. (h-k) B16-F1 or LLC cells expressing PMI-targeting or control shRNAs were injected into the flanks of C57BL/6 mice. Animals were maintained either with or without 20% mannose in drinking water and tumour growth was monitored over time (n=10 mice per group). (l) PMI expression levels in tissue microarrays from ovarian (n=45), renal (n=180), breast (n=159), prostate (Prost.)(n=155) and colorectal (Colorect.)(n=216) tumours. (m) Mice (n=14/group) were subjected to AOM/DSS treatment for 68 days. Animals were treated with normal drinking water or with 20% (w/v) mannose in the water until the end of the experiment. Tumours were counted in the colon of each mouse. (n) *VillinCre*^{ER} *Apc*$^{fl/+}$ *Kras*$^{G12D/+}$ mice were aged until clinical end-point. Mice were treated with normal drinking water or with 20% (w/v) mannose in water from four days post-induction until the end of the experiment (n=9 animals, - Mannose; n=8 animals, + Mannose). Tumours were counted in the colon of each mouse. n=3 independent experiments (b,c,e,f). n=5 independent experiments (d). Data represent one independeent experiment with technical triplicate (g) or are representative of two independent experiments (a). Data are mean +/- S.E.M.. Data analyzed by one-sided Mann-Whitney *U* test ***P < 0.001. Data

were analyzed in (c,e) by two-way ANOVA with Bonferroni correction, (d) multiple two-sided unpaired t-test with Holm-Sidak correction (h-k) two-way ANOVA with Tukey correction, (l) one-way ANOVA with Bonferroni correction and (m) unpaired two-tailed Student's t-test. *P < 0.05, **P < 0.01, ***P < 0.001. ****P < 0.0001

Methods (online-only)

Cell culture, transfections and infections

All cell lines were from Beatson Institute stocks and were originally obtained from ATCC, ECACC repositories apart from PATU-8902 (DMSZ, Cat#: ACC-179) and KP-4 ((RIKEN, Cat#: RCB1005). The following cells - A549, IGROV-1, Saos-2, U2OS, U2OS-E1a, SKOV-3, RKO, PATU-8902 – were grown in DMEM high glucose supplemented with 10% FBS, 0.292 mg/ml Glutamine and Penicillin (100 Units/ml)/Streptomycin (100μg/ml) (all from Life Technologies). U2OS-E1a cells generated in our laboratory and have been previously described[21]. K562 cells were grown in RPMI-1640 and KP-4 were grown in IMDM (Life Technologies) 20% FBS supplemented with Penicillin (100 Units/ml)/Streptomycin (100μg/ml). B16-F1 mouse skin melanoma cell line was a gift from Laura Machesky (Cancer Research UK Beatson Institute, UK) and were maintained in DMEM (Thermo Fisher Scientific, Cat#: 21969035) supplemented with 10% FBS (Thermo Fisher Scientific, Cat#: 10270106), 2 mM L-Glutamine (Thermo Fisher Scientific, Cat#: 25030032), and Penicillin-Streptomycin (Thermo Fisher Scientific, Cat#: 15140122). LLC mouse Lewis lung carcinoma cells were a gift from Sara Zanivan (Cancer Research UK Beatson Institute, UK) and were maintained in RPMI-1640 (Thermo Fisher Scientific, Cat#: 31870074), 10% FBS, 10mM HEPES (Thermo Fisher Scientific, Cat#: 15630080), 2mM L-Glutamine, and Penicillin-Streptomycin. These cell lines were confirmed to be free of mycoplasma.

Cells were transfected using Calcium Phosphate precipitates as previously described[16]. U2OS cells were infected with virus containing pBabe-puro-empty or pBabe-puro-Bcl-X_L following the same protocol as previously published[21]. U2OS cells were infected with virus containing

pLZRS empty or pLZRS HA-Mcl-1 (kindly provided by Stephen Tait)[22]. U2OS infected cells were selected in DMEM 10% FBS containing 600µg/mL of neomycin for 2 weeks. U2OS control and Bax/Bak CRISPR cells were kindly provided by Stephen Tait.

The following siRNAs were used:

PMI siRNA-1 (Dharmacon. catalog number: J-011729-05-0002),

PMI siRNA-2 (Dharmacon. catalog number: J-011729-06-0002),

PMI siRNA-3 (Dharmacon. catalog number: J-011729-07-0002),

PMI siRNA-4 (Dharmacon. catalog number: J-011729-08-0002).

NTC1 (Dharmacon. catalog number: D-001810-03-20),

NTC2 (Dharmacon. catalog number: D-001810-04-20.

lentiCRISPR v2 was a gift from Feng Zhang (Addgene plasmid #52961[23]. The following sgRNA sequences were used in the experiments.

NTC 1: GTAGCGAACGTGTCCGGCGT

NTC 2: GCTTGAGCACATACGCGAAT

ATG5: AAGAGTAAGTTATTTGACGT

ATG7: GAAGCTGAACGAGTATCGGC

Casp8 GCCTGGACTACATTCCGCAA

FADD TTCCTATGCCTCGGGCGCGT

BAX AGTAGAAAAGGGCGACAACC

BAK GCCATGCTGGTAGACGTGTA

NOXA TCGAGTGTGCTACTCAACTC

pGIPZ-non-targeting control (NTC) (Cat#: RHS4346), PMI #1 (Cat#: RMM4431-200352145, Clone ID: V2LMM_110673), and PMI #2 (Cat#: RMM4431-200355616, Clone ID: V2LMM_203337) shRNAs were purchased from Dharmacon.

pLX304 was a gift from David Root (Addgene plasmid #25890). Human PMI cDNA was amplified using pCMV-Sport-MPI (Dharmacon cat no: MHS6278-202802339) as a template and inserted into pDONR221 vector (Thermo Fisher Scientific, Cat#: 12536017) using Gateway BP Clonase II Enzyme mix (Thermo Fisher Scientific, Cat#: 11789020). PMI cDNA was then transferred into pLX304 destination vector using Gateway LR Clonase II Enzyme mix (Thermo Fisher Scientific, Cat#: 11791020).

Lentivirus production and infection were carried our as described before[24].

Cell culture treatments.

Mannose treatment

Cells were seeded in 6-well plates and incubated overnight at 37^0C. The following day, the medium was replenished with fresh full growth medium (DMEM, RPMI or IMDM) containing 25mM Mannose (when DMEM or IMDM) or 11.11mM Mannose (when RPMI). Other sugars were added at 25mM concentration: D-glucose (Sigma, G8270), D-fructose (Sigma F3510), D-galactose (Sigma G5388), L-Fucose (Sigma F2252 and Cayman chemical 16479). New stocks were prepared every two weeks of 1M Mannose in milliQ water and sterilised by filtering through a 0.22µm pore filter. For control conditions, the same volume of milliQ water was added to the medium. Cells were left for at least 24 hours for cell death experiments or for 6 hours for metabolic experiments. Cell death was blocked by treatment

with zVAD-fmk (Apax Labs, A1902). 2-Deocy-D-glucose (Sigma-Aldrich, Cat#: D8375), Tunicamycin (Sigma-Aldrich, Cat#: T7765), Chloroquine (Sigma-Aldrich, Cat#: C6628).

^{13}C-labelled sugars

Cells were seeded and the following day washed 3 times with abundant PBS before adding glucose-free DMEM (supplemented with 10% dialyzed FBS, 2mM glutamine, 100 Units/ml of penicillin and 100 μg/ml of streptomycin). This medium could contain 5mM of 1,2-$^{13}C_2$-glucose alone, together with $^{13}C_6$-mannose or 5mM $^{13}C_6$-mannose alone. Stocks of 1,2-$^{13}C_2$-glucose and $^{13}C_6$-mannose were prepared at a concentration of 0.5M in milliQ water prior to sterilization by filtering through a 0.22μm pore filter.

Chemotherapeutic drugs

Cells were plated overnight and were then incubated for the times indicated in control or mannose-containing medium. After one day incubation, fresh control and mannose-containing media were prepared and drugs were added as described for each experiment. Drugs used were: Cisplatin (Sigma; C2210000), doxorubicin (Sigma; D1515).

Western blotting

Protein extraction was performed as previously described[25]. Protein lysates were separated by SDS-PAGE and blotted onto Nitrocellulose membranes. Western blot analysis was performed according to standard techniques as previously described[25]. The following antibodies were used at a 1/1000 dilution unless otherwise stated: β-Actin (Abcam; ab8227), Mcl-1 (Cell signaling; 4572), ERK2 (Santa Cruz; sc-154), Bcl-X_L (Cell signaling; 2762), HSP-90β (Santa Cruz; sc-1057), PARP (Cell signalling; 9542), Cleaved-caspase-3 (Cell signalling; 9664), FADD (Transduction labs; F36620), Caspase-8 (Cell signalling; 4790), Bax (Transduction labs; 610983), Bak (Cell signalling; 6947), Bim (Cell signalling; 2993),

Noxa (Novus Biologicals; NB-600-1159), phospho-AMPKα (Cell signalling; 2535), AMPKα (Cell signalling; 5832), PMI (Abcam; 128115). LC3B (Cell Signaling Technology, Cat#: 2775S, 1/1500), β-actin (Cell Signaling Technology, Cat#: 4670S, 1/2000), ATG5 (Cell Signaling Technology, Cat#: 12994S), ATG7 (Cell Signaling Technology, Cat#: 8558S), Bip/GRP78 (Cell Signaling Technology, Cat#: 3177S), p62 (BD Biosciences, Cat#: 610833, 1/2000). Mouse PMI protein was detected using rabbit polyclonal PMI antibody (Proteintech, Cat#: 14234-1-AP). Validation was based on information provided in manufacturers' datasheets. In addition, as indicated in the manuscript, we utilized RNAi or CRISPR/Cas9 to validate the following the antibodies used to detect the following proteins: Bax, Bak, Caspase-8, FADD, PMI, Atg5 and Atg7.

Metabolic extraction of intracellular metabolites

Cells were seeded at a concentration of 100,000 cells/well in 6-well plates. The next morning, the medium was replenished with fresh full medium and cells were kept under this condition for another 24 hours to stabilise their metabolism. Approximately 36-40 hours after being plated, cells were treated under different conditions as described in results, using full growth medium or glucose-free with or without the presence of unlabelled sugars or labelled sugars for 6 hours. After 6 hours incubation at 37^{o}C, intracellular metabolites were extracted.

Medium was aspirated and 6-well plates were placed on ice and washed thoroughly with 4^{0}C PBS 3 times before addition of 500µL extraction solvent (50% Methanol, 30% Acetonitrile, 20% milliQ water) to each well. Plates were then agitated at 4^{0}C for 5 min to successfully extract intracellular metabolites and then centrifuged at 16,100g for 10 min at 4°C. Supernatants were transferred into HPLC vials and stored at -80°C prior to LC-MS analysis.

An Exactive Orbitrap mass spectrometer (Thermo Scientific, Waltham, MA, USA) was used together with a Thermo Scientific Accela HPLC system. The HPLC setup consisted of a ZIC-pHILIC column (SeQuant, 150 x 2.1mm, 5µm, Merck KGaA, Darmstadt, Germany), with a ZIC-pHILIC guard column (SeQuant, 20 x 2.1mm) and an initial mobile phase of 20% 20mM ammonium carbonate, pH 9.4, and 80% acetonitrile. Cell extracts (5µl) were injected and metabolites were separated over a 15 min mobile phase gradient, decreasing the acetonitrile content to 20%, at a flow rate of 200µL/min and a column temperature of 45°C. The total analysis time was 23 min. For longer runsd of 37 min, a 30 min gradient with the same solbenst was used, at a flow rate of 100µL/min and a column temperature of 30°C[26]. All metabolites were detected across a mass range of 75-1000 m/z using the Exactive mass spectrometer at a resolution of 25,000 (at 200m/z), with electrospray (ESI) ionization and polarity switching to enable both positive and negative ions to be determined in the same run. Lock masses were used and the mass accuracy obtained for all metabolites was below 5ppm. Data were acquired with Thermo Xcalibur software (version 2.2).

The peak areas of different metabolites were determined using Thermo TraceFinder software (version 3.2) where metabolites were identified by the exact mass of the singly charged ion and by known retention time on the HPLC column. Commercial standards of all metabolites detected had been analysed previously on this LC-MS system with the pHILIC column. The ^{13}C labelling patterns were determined by measuring peak areas for the accurate mass of each isotopologue of many metabolites. Intracellular metabolites were normalized to protein content of the cells, measured at the end of the experiment by the Lowry assay [27]. As the proteins have precippitated on the addition of the metabolite extraction solvent, protein contents are measured in the exact same wells as the metabolites have been extracted.

Translation assay

Cells at 50% confluency were pretreated with or without 25mM mannose for 24h or with 100μg/ml cycloheximide for 1 hour. 1MBq ^{35}S methionine (Perkin Elmer, EasyTag™ EXPRESS^{35}S Protein Labeling Mix, cat no NEG772002MC) was added to the culture medium, 2ml/well, 6 well plate for 30 min. Cells were washed in ice cold PBS, then lysed in lysis buffer (10mM Tris pH 7.5, 50mM NaCl, 0.5% NP40, 0.5% SDS, benzonase (Sigma cat no: E1014, 2ul/10ml lysis buffer). Proteins were precipitated in 25% trichloroacetic acid (TCA) at 4^{o}C for 30 minutes. TCA precipitates were washed on glass fibre filters (Whatman 934-AH, cat no 1287-024) with 70% ethanol then acetone and dried and ^{35}S incorporation quantitated in a liquid scintillation counter. Results were calculated as relative ^{35}S incorporation/10^5 cells.

Transcription assay

Cells at 50% confluency were pretreated with or without 25mM mannose for 24h or with 5μM Actinomycin D for 1 hour. 1.1MBq ^{32}P UTP (Perkin Elmer, cat no:BLU007H001MC) was added to the culture medium, 2ml/well, 6 well plate for 6 hours. Cells were washed in PBS and mRNA prepared using the Dynabeads mRNA DIRECT Kit (Life Technologies, cat no:61012). ^{32}P labelled mRNA was quantitated in a liquid scintillation counter and results were calculated as relative ^{32}P UTP incorporation/10^5 cells.

PMI enzymatic assay

Cells were grown to confluence, washed with PBS and collected by centrifugation 5 min 150 x g. at 4 C. Cell pellets were lysed by 3 freezing/thawing cycles. 40μg of post-nuclear protein fractions were used to determine PMI activities in each cell line tested by means of a coupled enzymatic reaction. Briefly, samples were incubated in a buffer containing 200mU of Phosphoglucose isomerase (PGI) (Roche, cat#10 127 396 001), 500mM Glucose 6 phosphate

dehydrogenase (G6PDH), 1mM NADP +, 40mM Tris-HCl, pH 7.4, 6 mM MgCl2, 5 mM Na_2HPO_4/KH_2PO_4. Reactions were initiated by addition of 1mM mannose 6 phosphate, and the production of $NADPH/H^+$ was assessed for 2h at room temperature by measuring the O.D at 340nm. In parallel, western blots directed against PMI and ERK2 were performed to examine the correlation between PMI activities and PMI expression levels in each cell line analysed.

Proteasome assay

Cells were seeded 24h prior to 24h treatments using media supplemented or not with 25mM mannose. A luminescence-based assay (Proteasome-Glo™ Chymotrypsin-like Cell-based Assays, Promega) was performed according to manufacturer's protocol. The measured proteasome activities were normalised to cell number by counting cells at the end of each experiment. Cells were treated with 10μM MG132 as a control for the specificity of the assay.

Lowry assay

Lowry assay was used to determine the total protein content for each one of the triplicates from the metabolic experiments. First, 500μL of solution A (70% milliQ water, 20% NaOH 5N, 10% 2,5-Dimethoxy-4-chloroamphetamine) were added to each well from a 6-well plate and left under agitation for 20 min. After this, 5mL of solution B (0.5g NaCu-EDTA, 40g Na_2CO_3, 8g NaOH for 2 litres) were added to each well and left for 40 min. Lastly, 500μL of Folin reagent were added to each well and left for a minimum of 15 min until colour blue is observed in each well. Also, one or two 6-well plates were used for generation of a protein concentration standard curve with BSA.

Finally, 200µL of each well were separately transferred to a 96-well plate and absorbance was measured at 750nm. Then, protein concentration was measured by calculating the equation of the standard curve and extrapolating the absorbance of each well.

Flow cytometry

Flow cytometry for unfixed cells (cell death assay) was conducted as previously described[28], and a FACSCalibur or ATTune NXT flow cytometer was used for the analysis.

Animal experiments

All in vivo xenograft experiments were performed using 6-week old female CD1-nude mice or C57/BL6J wild-type mice as approved by the Glasgow University Animal Welfare and Ethical Review Body and in accordance with UK Home Office guidelines. Mice were placed 5 per cage with access to water and food (chow diet) *ad libitum*. Experimental cohort sizes were based on previous similar studies that have given statistical results while also respecting limited use of animals in line the 3R system: Replacement, Reduction, Refinement. In no case were animals maintained once the tumour size limit permitted in our Home Office license (15mm in any diretion) was reached. All treatment studies were randomized, but did not involve blinding.

KP-4 cells were injected subcutaneously with 100µL of matrigel containing 5 million cells in either the right flank or both left and right flanks. LLC and B16-F1 cell were injected sucutaneously in PBS suspension with 200µL (LLC, $1x10^6$ cells) and 100µL (B16-F1, $1x10^6$ cells) Mice were weighted and tumours were measured using callipers thrice per week (usually on Monday, Wednesday and Friday of each week). Calculation of tumour volume was as follows: (L x S2)/2 (L: longest length; S: shortest length).

For mannose treatment, normal drinking water was exchanged for 200mL of 20% mannose in drinking water (w/v) and it was replaced once every week. Mice received mannose by oral gavage (200μL) 3 times per week from the same stock of 20% mannose in water.

For doxorubicin treatments, mice received intraperitoneal injections at a concentration of 5mg/kg for each mouse once per week. Stocks of 1mg/mL doxorubicin (Sigma, D1515) were prepared in milliQ water.

For azoxymethane (AOM) / dextran sodium sulphate (DSS) experiments, mice were injected with a single dose of AOM (Sigma, A5486) at 10mg/kg. Five days after AOM injection, mice received 3 cycles of 1.5% DSS (MP Biomedical, 0216011080) in water for 5 days per cycle with one week in between each cycle. In the week between each cycle, mice received normal water or 20% (w/v) mannose water. After the last cycle of DSS, mice were kept with normal water or mannose for two weeks before being culled at day 68.

Tissue harvest

All mice were culled by CO_2 mediated euthanasia[29] before harvesting any tissue sample. Mice were put in a cage for exposure to CO_2 for 100 seconds before neck dislocation.

Xenografted tumours were removed and detached from the skin and cut in half. One half of each tumour was fixed for 24-30 hours in 10% neutral buffered formalin at room temperature. Formalin was then exchanged for 70% ethanol prior to histology.

The colons of mice from AOM/DSS carcinogenesis experiments were collected and fixed in formalin for histological processing.

For CRC GEMM – male and female *VillinCre*^{ER} *Apc*$^{fl/+}$ *Kras*$^{G12D/+}$ mice[30] aged 6-12 weeks were given a single intraperitoneal injection of 80m/kg tamoxifen (Sigma, T5648). Four days

post-induction drinking water was excahnged for 20% mannose in drinking water (w/v) or given drinking water *ad libitum*, this was replaced every week. Mice were aged until clinical end-point – when they displayed anaemia, hunching or weight loss. Colons were pinned out into 10% neutral buffered formalin and the number of colons counted.

Blood sampling and blood metabolic extraction

To measure blood mannose levels tail tipping was performed. Blood samples were directly frozen using dry ice and stored at -80^{0}C until metabolic extraction was performed.

For metabolic extraction of whole blood, 2-5µL of each sample were diluted in 100-250µL of metabolic extraction buffer on ice for 5 min (1:50 dilution). Then, all samples were centrifuged at 13000rpm at 4^{0}C for 15 min. Finally, 100µL of the supernatant from each sample was transferred into HPLC vials and stored at -80°C until LC-MS analysis.

PET-MRI scanning

Mice with KP-4 cells xenografts (n=9, weight 24.6±1.8g) received either 200µL of 20% w/v mannose in water (treatment group) or normal water (control group) by oral gavage 20min before ^{18}F-FDG injection. ^{18}F-FDG (12.9±1MBq) in 200µl of normal saline was administered via an intravenous (i.v.) bolus injection in tail vein. After an uptake phase of 30 min, positron emission tomography (PET) and magnetic resonance imaging (MRI) scans were sequentially performed using a nanoScan (Mediso Ltd.) PET/MRI (1T) scanner. Mice were maintained under 2-2.5% isoflurane in medical air during injection and imaging procedures periods. Static PET acquisitions were performed for 15 min and after that whole body T1 GRE 3D Multi-FOV MRI scans (slice thickness 0.50mm, repetition time (TR) 10msec, Echo time (TE) 2.3msec, flip angle 12 degress) performed to obtain anatomical references. For quantitative assessments of scans, regions of interest (ROI) were manually drawn around the

edge of the tumour xenograft on MRI scans by visual inspection using PMOD software version 3.504 (PMOD Technologies Ltd.) and same ROI copied on respective PET scans. Tumours ROIs were slightly different between scans depending on the positions and angles of the mice on the scanner therefore separate ROIs for each scan were drawn. The percentage injected dose per gram (%ID/ml) was calculated using formula: %ID/ml = ROI activity (kBq/ml) divided by injected dose multiplied by 100%. Data were reported as average % ID/ml $\pm$ SD. Student's t-tests were used when comparing data between mannose treated and control mice.

Immunohistochemistry – Tissue Microarray PMI staining

TMAs were first placed in xylene for 5 min before three washes for 1 min each (two in ethanol and one in 70% ethanol). TMAs were washed for 5 min in deionised water before 25 min at 98°C in PT module pH 6 sodium citrate retrieval buffer. They were further washed once in tris buffered tween (TbT) before blocking endogenous peroxidase for 5 min. TMAs were washed again using TbT and stained with PMI antibody (1C7) 1/50 dilution for one hour. TMAs were washed in TbT before and after 30 min on Mouse EnVision. 10 min incubation in 3,3'-diaminobenzidine tetrahydrochloride was perfomed. TMAs were again washed with dionised water (for 1 min) before and after Haematoxylin Z incubation with post-incubation with 1% acid alcohol. This was followed by a 30 seconds wash with dionised water followed by 1 min incubation with scotts tap water substitute and another minute with dionised water.

Immunohistochemistry – BrdU staining

Xenografted tumours were embedded in paraffin and cut in sections at appropiate thickness before placing the section at 60°C overnight. Sections were first placed in xylene for 5 min

before three washes for 1 min each (two in ethanol and one in 70% ethanol). Sections were washed for 5 min in deionised water before 25 min at 98ºC in PT module pH 6 sodium citrate retrieval buffer. They were further washed once in tris buffered tween (TbT) before blocking endogenous peroxidase for 5 min. Sections were washed in TbT before and after incubation with BrdU antibody (BD Biosciences #347580, 1/200 dilution) for 35 min. Sections were washed in TbT before and after 30 min on Mouse EnVision. 10 min incubation in 3,3'-diaminobenzidine tetrahydrochloride was perfomed. Sections were agains washed with dionised water (for 1 min) before and after Haematoxylin Z incubation with post-incubation with 1% acid alcohol. Quick wash of 30 seconds with dionised water followed by 1 min incubation with scotts tap water substitute and another minute with dionised water.

Tissue Microarrays

TMAs from ovarian, breast, colorectal, prostate and renal cancer were stained for phosphomannose isomerase (PMI). TMAs were scanned using Leica Biosystems and were scored for PMI expression based on the percentage of tumour that showed negative, low, medium or high expression. Each sample was scored with a number between 0-300 following this equation: Score=(0 x negative) + (1 x low) + (2 x medium) + (3 x high).

Statistical analysis and Reproducibility.

All data presented were analysed using GraphPad Prism software. Three different statistical analyses were performed depending on the data from the different experiments shown. Generally, one-way ANOVA, two-way ANOVA, Log-Rank (Mantel-Cox) test and Student's t-test that could be paired or unpaired and one-tailed or two-tailed. Three levels of significance were determined: *$p < 0.05$, **$p < 0.01$, ***$p < 0.001$, ****$P<0.0001$, ns = no

significant. Where a representative experiment is shown, the number of times the same result was observed in independent experiments is detailed in the corresponding figure legend.

Data Availability

Data that support the findings in this study are stored at the Cancer Research UK Beatson Institute and are available from the corresponding author upon reasonable request.

Extended Data Figures:

Extended Data Figure 1: (a**)**. Growth curves of Saos-2 cells supplemented without (Ctrl) or with 25mM of hexoses (Man, mannose; Gal, galactose; Fru, fructose; Fuc, fucose; Glc, glucose). (b-d) Growth curves of (b) PA-TU-8902 and (d) A549 cells in DMEM (-Man) or with additional 25mM mannose (+Man); (c) K562 cells in 10% FBS RPMI medium with or without 11.1mM mannose. (e) Western blotting showing the levels of phospho-AMPKα (T172) and total AMPKα after 5, 15, 30 and 45 min incubation of U2OS with 25mM mannose-supplemented or regular medium. (f) Growth curves of SKOV3 and RKO cells in DMEM (-Man) or with additional 25mM mannose (+Man). (g) Levels (peak area per microgram of protein) of 2-deoxyglucose-phosphate (2-DG-P) in RKO, SKOV3, SAOS-2 and U2OS cells incubated with 10mM 2-deoxyglucose for 6h in the presence of 25 mM mannose in the culture medium (DMEM). Data represent the average of three technical replicates. (h) Percentage of peak area per microgram of protein (log-10 scale) of hexoses-6-phosphate in U2OS cells after 6h incubation in 10% dialyzed FBS 5mM glucose DMEM with or without 5mM mannose. (i) Peak area per microgram of protein of hexoses-6-phosphate in U2OS cells incubated for 6 hours in DMEM with or without additional 25mM of sugars (Man, mannose; Gal, galactose; Fru, fructose; Fuc, fucose; Glc, glucose). (j,k) Peak area per microgram of protein of intracellular non-phosphorylated (j) mannose or (k) glucose after 6 hours incubation of U2OS cells in 5mM glucose DMEM with or without 5mM mannose. (l) Peak area per microgram of protein of non-phosphorylated glucose m+2 after 6 hours incubation of U2OS cells in glucose-free DMEM with 5mM 1,2-$^{13}C_2$-D-glucose alone and with or without 5mM $^{13}C_6$-D-mannose. (m-p) Peak area per microgram of protein of (m) glyceraldehyde-3-phosphate (GA3P), (n) phosphoenolpyruvate (PEP), (o) lactate and (p) UDP-N-Acetyl-glucosamine (UDP-GlcNAc) in U2OS cells after 6 hours incubation in

DMEM with or without additional 25mM of other sugars (Man, mannose; Gal, galactose; Fru, fructose; Fuc, fucose; Glc, glucose). n=3 independent experiments (a,b,c,d,f,h,i,j,k,l,m,n,o,p). Data are representative of 2 independent experiments (e). In all data error bars represent mean +/- S.E.M.. Data were analysed by (i,m,n,o,p) one-way ANOVA, (a) two-way ANOVA followed by Tukey's multiple comparisons or (h,j,k,l) paired two-tailed Student's t-test. *P < 0.05, **P < 0.01, ***P < 0.001.

Extended Data Figure 2: (a) Levels (peak area per microgram of proteins) of 2-deoxy-2-fluoro-D-mannose-phosphate (2-DFM-P) in RKO, SKOV3, SAOS-2 and U2OS cells after 6 hours treatment with or without 2mM 2-deoxy-2 fluoro-D-mannose. Relative levels of exoses-6-phosphate (b), lactate (c), glyceraldehyde-3-phosphate (d), phosphoenolpyruvate (e), malate (f), ribose-5-phosphate (g) uridine diphosphate N-acetylglucosamine (UDP-GlcNac) (h) in SKOV3 and U2OS cells after 6 hours treatment with (+ Man) or without (- Man) 25 mM mannose in the culture medium (DMEM). Data in (a) represent the average of three technical replicates. (b-h) n=2 independent experimenst (each involving technical triplicates). In all data error bars represent mean +/- S.E.M..

Extended Data Figure 3:

Content (peak area per microgram of proteins) of (**a**) Hexoses-6-phosphate (Hexoses-6P), (**b**) ATP, (**c**) AMP, (**d**) Fructose 1,6-bisphosphate (F1,6-BP), (**e**) Ribose-5-phosphate (Ribose 5P) and (**f**) uridine diphosphate N-acetylglucosamine (UDP-GlcNac) in U2OS cells after 5 minutes treatment with (+ Man) or without (- Man) 25 mM mannose in the culture medium

(DMEM). n=3 independent experiments, presented as mean ± S.E.M. and analyzed by two-tailed unpaired t-test. *P < 0.05, ***P < 0.001.

Extended Data Figure 4: (a-b) Percentage of PI-positive KP-4 cells after 24 h treatment with (a) 40μM cisplatin or (b) 1μg/mL doxorubicin in the presence or absence of 25mM mannose. (c) Percentage of U2OS PI-positive cells after 24 h treatment with or without 10μM cisplatin in DMEM with or without 25mM of additional sugars (Man, mannose; Gal, galactose; Fru, fructose; Fuc, fucose; Glc, glucose). (d) Percentage of U2OS PI-positive cells after 24 h treatment with or without 1μg/mL doxorubicin, with or without 25mM mannose and with or without 50μM zVAD-fmk. (e-f) Fold increase of the percentage of PI-positive Saos-2 (NTC, caspase-8 and FADD CRISPR) cells upon 24 hours treatment in DMEM with or without 1μg/mL doxorubicin (e) or 10μM cisplatin (f) and with or without 25mM mannose. (g) Western blotting showing the levels of caspase-8, FADD and ERK2 in NTC, caspase-8 and FADD CRISPR Saos-2 cells. (h) Percentage of Empty and Bax/Bak CRISPR U2OS PI-positive cells with or without 1μg/mL doxorubicin and with or without 25mM mannose. (i) Western blotting showing the levels of Bax, Bak and HSP90 in Empty and Bax/Bak CRISPR U2OS cells. (j) Western blot showing the levels of Bim, Noxa, Bad, Bax, Actin and HSP-90 in U2OS cells after 24 hours treatment with or without 10μM cisplatin, with or without 25mM mannose and with or without 50μM zVAD-fmk. The HSP-90 blot is identical to the one shown in Fig 2h as the the blots are from the same experiment. (k) Western blotting showing the levels of Mcl-1 and Bcl-X_L in U2OS cells after 48 h with or without 10μM cisplatin, with or without 25mM mannose and in the absence or presence of 10μM MG132 as indicated. (l-m) qRT-PCR showing the levels of (l) *BCL2L1* (Bcl-X_L) and (m) *MCL1* mRNAs in U2OS cells after 48 h treatment with or without 10μM cisplatin, with

or without 25mM mannose in the presence of 50μM zVAD-fmk. (n-o) Percentage of U2OS Emtpy, Mcl-1 and Bcl-X_L overexpressing PI-positive cells after 24 hours treatment with or without 1μg/mL doxorubicin and with or without 25mM mannose. (p-q) Western blot showing the levels of Mcl-1, Bcl-X_L and HSP-90 in U2OS Emtpy, Mcl-1 and Bcl-X_L overexpressing cells. n=3 independent experiments (a,b,c,e,f,h,l,m,n,o). Data are representative of two independent experiments (g,j,k) or one experiment (i,p,q). In (d), n =3 independent experiments (each involving technical triplicates) (-zVAD-fmk) and n=2 independent experimenst (each involving technical triplicates) (+zVAD-fmk). In all data, error bars represent mean +/- S.E.M.. Data were analysed by (a,b,c,d,e,f,h,n,o) two-way ANOVA with Bonferroni correction. *P < 0.05, **P < 0.01, ***P < 0.001.

Extended data Figure 5: Sensitization to cell death by mannose is connected to Bcl-2 family memebers. (a) Percentage of control (NTC) and Noxa CRISPR U2OS PI-positive cells upon 24h treatment with or without 10μM cisplatin and with or without 25mM mannose. (b) Percentage of U2OS PI-positive cells upon 24hr treatment with 10μM WEHI539, a BclX_L inhibitor, or 10μM ABT-199, a Bcl-2 inhibitor, with or without 25mM mannose. n=4 independent experiments (a) or n=3 three independent experiments (b). In all data. error bars represent mean +/- S.E.M.. Data were analyzed by two-way ANOVA with Bonferonni correction (a) and two-tailed unpaired t-test (b). ****P<0.0001; ns, not significant.

Extended data Figure 6: (a) Mannose levels in the plasma after 60 min in mice treated with a single dose of 200μL of water (-Man) or 20% mannose in water (w/v) (+Man). (b-c) CD1-

nude mice were transplanted with KP-4 cells subcutaneously and tumours were grown for 14 days. PET-MRI scans were performed for mice treated with 200µL of water (-Man) or 20% (w/v) mannose in water (+Man) by oral gavage 20 min before ^{18}F-FDG tail vein injection. (b) Quantification of ^{18}F-FDG uptake by tumours represented in average % ID/mL +/- SD. (c) Tumour volume (mm^3) of each tumour at the moment of the PET-MRI scan. Data were analyzed by unpaired two-tailed Student's t-test. (d) CD1-nude mice were injected with KP-4 cells subcutaneously and treated with normal drinking water (-Man) or 20% mannose in the drinking water (w/v) plus the same treatment via oral gavage 3 days per week from the 3rd day after tumour transplantation. Shown is the quantification of ^{18}F-FDG uptake by tumour and different organs represented in averaged kBq/mL +/- SD. Data were analyzed by unpaired two-tailed Student's t-test. (e) CD1-nuce mice were injected with KP-4 cells subcutaneously and treated with normal drinking water (-Man) or 20% mannose in the drinking water (w/v) plus the same treatment via oral gavage 3 days per week from the 3rd day after tumour transplantation. Mouse weights were recorded at the indicated times. (f,g) CD1-nuce mice were injected with KP-4 cells subcutaneously and treated with normal drinking water (-Man) or 20% mannose in the drinking water (w/v) plus the same treatment via oral gavage 3 days per week from the 3rd day after tumour transplantation. Images of BrdU sections representing tumours in control (-Man) and mannose-treated (+Man) mice (f). (g) Quantification of BrdU-positive cells per section in n=4 control tumours (-Man) and n=4 mannose-treated tumours. 5 representative pictures per tumour were analysed. (h) CD1-nude mice were injected with KP-4 cells subcutaneously and tumours were grown for 10 days before treatment mannose (Man) and/or doxorubicin (Doxo) was started. Mice received normal drinking water (Ctrl and Doxo) or 20% mannose in the drinking water (Man and Doxo + Man) together with the same treatment by oral gavage thrice per week. Doxorubicin treatment started on day 32 and mice received 5mg/kg by IP injection once per week. Mouse

weight in all groups throughout the experiment (h). Mice number for each experiment is (a) n=3 animals per group, (b-d) n=5 animals per group, -Man; n=4 animals per group, +Man, (h) n=10 animals/group. In a,c and h error bars represent mean +/- S.E.M.. Data were analysed with a two-tailed unpaired t-test (c). *P < 0.05, **P < 0.01

Extended data Figure 7: (a) PMI expression levels correlate with PMI activities. PMI activities were measured in 8 different cell lines using coupled enzymatic reactions. Graph shows the OD_{340nm} measured at 2h reflecting the amount of NADPH/H+ produced by the reactions. Results from 3 independent experiments were normalised relative to PMI activities measured in Saos-2 cells and represent means +/- SEM. (b-g) PMI knockdowm senstizes cells to mannose. (b) Western blot of SKOV3 transfected cells showing the levels of PMI and actin after 48 h of transient transfection with siRNAs. Growth curves of (c) SKOV3, (f) RKO and (g) IGROV1 in regular DMEM supplemented with or without 25mM mannose after transient transfection for 48 hours with 2 NTC and 2 PMI targeting siRNAs. (d,e) Western blot showing the levels of PMI and ERK2 in (d) RKO and PMI and actin in (e) IGROV1 48h post siRNA transfection. (h-k) Over-expression of PMI causes resistance to the growth suppressing and death–promoting effects of mannose. PMI expression in U2Os (h) and Saos- (i) was confirmed by western blotting. (j) Saos2-PMI cells and Control cells (Saos-2) were plated in the presence (+Man) or the absence (-Man) of 25mM mannose and cell numbers counted at the times indicated. (k) Percentage of PI-positive U2OS control cells (V) or U2OS cells overexpressing PMI (PMI) after 24h treatment with or without 1μg/ml doxorubicin in the presence or absence of 25mM mannose. (l-o) Percentage of (l) lactate, (m) glyceraldehyde-3-phoshate (GA3-P), (n) α-ketoglutarate (α-KG) and (o) malate metabolic content in SKOV3 transfected cells with siRNA for 48 hours before 6 h incubation

in complete DMEM medium with or without supplementation of 25mM mannose. n=3 independent experiments (a,c,f,g,j,l,m,n,o). Data are representative of two independent experiments (b,d,e,k), or one experiment (h,i). In all data, error bars represent mean +/- S.E.M.. Data were analyzed by (a) two-tailed unpaired t-test (l,m,n,o) two-way ANOVA with Tukey correction, (j) Multiple unpaired two-sided t-test with Holm-Sidak correction. *P<0.05, ***P<0.001, ****P < 0.0001.

Extended Data Figure 8: (a-b) PMI knockdown causes growth retardation upon mannose treatment in a dose-dependent manner. B16-F1 cells infected with non-targeting control (NTC) or PMI shRNA were treated with (blue columns) or without (white columns) 25mM mannose for 72h when cell number was then determined (a) Results are shown as mean ± S.E.M. n=3 independent experiments. PMI knockdown was confirmed by western blotting (b). (c) Western blot showing PMI knockdown in LLC cells. The data are relative to the experiment shown in Figure 4c. (d) B16-F1 cells infected with non-targeting control (NTC) or PMI shRNA were treated with 25 mM Mannose (Man), 25 mM Glucose (Glc), 25 mM Galactose (Gal), 25 mM Fructose (Fru), 25 mM Fucose (Fuc). At 24, 48, and 72h after hexose treatment, cell number was determined. The results are shown as mean ± S.E.M.. (e-h) Weights of mice injected with syngeneic cells lines: B16 shNTC (e), B16 shPMI (f), LLC shNTC (g) and LLC shPMI (h) which had been given drinking water (-Man) or drinking water supplemeneted with 20% mannose (+Man) (n=10 mice per group). All date are mean +/- S.D. unless otherwise stated. In d) n=4 independent experiments which were analysed by two-way ANOVA followed by Tukey's multiple comparisons. The data in b and c were only performed once. ***P<0.001

Extended data Figure 9: (a) Images of PMI expression for each TMA representing one negative sample, one low expression and one high expression. One sample came from each of the ovarian, breast, prostate, colorectal or renal TMAs. (b,c) Kaplan Meier curves showing cancer specific survival based on PMIlevles in (b) n=698 patients with stage I-IV colorectal cancer or (c) n=316 patients with primary operable breast cancer. (d) Table showing association of PMI and cancer specific survival. Histoscores were split into high and low expression using the ROC curve analysis for each tumour type. Log-rank analysis (two-sided) was used to compare PMI and cancer specific survival using SPSS (version 22). (e) Weight of 28 mice during the treatments of AOM/DSS with or without additional mannose treatment. (f) Weight of aged *VillinCre*^{ER} *Apc*$^{fl/+}$ *Kras*$^{G12D/+}$ mice during treatment with or without mannose. Data represented as mean of each group (n=7 animals, - Man; n=8 animals, + Man).

Extended Data Figure 10: Mannose does not affect amino acid and fatty acid uptake nor does it significantly affect serine and glycine levels, ER stress or proteasome activity, but it does affect autophagy, transcription and translation in a PMI-dependent manner. (a) Exchange rates of amino acids between the indicated cells and their media measured after 48 hours treatment with (+ Man) or without (- Man) 25 mM mannose. Results are presented as Peak Area per micrograms of proteins per hour and are representative of one experiment. Shown is the mean of 6 technical replicates. (b) Levels of $^{13}C_{16}$-Palmitate (expressed as peak area per micrograms of proteins) in U2OS cells incubated with 50 µM $^{13}C_{16}$-Palmitate, conjugated with 10% fatty acids-free bovine serum albumin (BSA), for 24 hours in the presence (+) or absence (-) of 25 mM mannose in the culture medium (DMEM). n=2 independent experiments (each involving 6 technical replicates). Data are presented as

mean ± S.E.M. Levels of $^{13}C_3$-Serine (c) and $^{13}C_2$-Glycine (d) (expressed as peak area per micrograms of proteins) in U2OS cells incubated with 25 mM $^{13}C_6$-Glucose for the indicated time in the presence (+ Man) or absence (- Man) of 25 mM mannose in the culture medium (DMEM). n=3 independent experiments. Isotopologues distribution of intracellular Serine (e) and Glycine (f) in U2OS cells incubated with 25 mM $^{13}C_6$-Glucose for 24 hours in the presence (MANNOSE) or absence (CTR) of 25 mM mannose in the culture medium (DMEM). n=3 independent experiments. (g) Mannose has no effect on the unfolded protein response. U2OS E1A cells were treated with 25 mM D-(+)-Mannose (Man) for 16 and 24 h. 2-Deoxy-D-glucose (2DG) and Tunicamycin (TM) serve as positive controls. Induction of Bip/GRFP78 (Bip) is a readout of ER stress. The data are representative of three independent experiments. (h) Proteasome activity is not affected by mannose. Mannose-sensitive U2OS cells were incubated in either DMEM or DMEM containing 25 mM mannose prior to measurement of proteasome activities. Cells were also treated with10 μM MG132 as a control for proteasome activity. n=3 independent experiments. (i,j) U2OS cells (i) or U2OS cells over-expressing PMI (j) were treated with 25 mM D-(+)-Mannose (Man) for the indicated times in the presence or absence of 20 μM Chloroquine (CQ) (4 hr). Western blotting was undertaken to detect LC3-B and actin. The data are representative of three independent experiments. (k,l) Relative incorporation of ^{32}P UTP (k) or ^{35}S methionine (l) into U2OS control cells (vector) or U2OS cells overexpressing PMI (PMI) in the presence or absence of 25mM mannose. Where indicated 5μM Actinomycin D was used to inhibit transcription or 100μg/ml cycloheximide was used to inhibit translation. (m,n) U2OS E1A cells infected with lentiCRISPR-NTC 1, NTC 2, ATG5, or ATG7 were treated with 25 mM D-(+)-Mannose (Man) for 72h before cell counting (m). The results are shown as mean and represent representative one independent experiment performed in triplicate. (n) Western

blots show loss of LC3 lipidation and p62 accumulation in ATG5 and ATG7 knockout cells. In k, n= 3 independent experiments. In l n=3 independent experiments (control and mannose) and n=2 independent experiments (CHX). Data were analyzed by two-tailed unpaired t-tests. *P<0.05, ***P<0.001. Unless otherwise stated, data respresent mean +/- S.E.M..

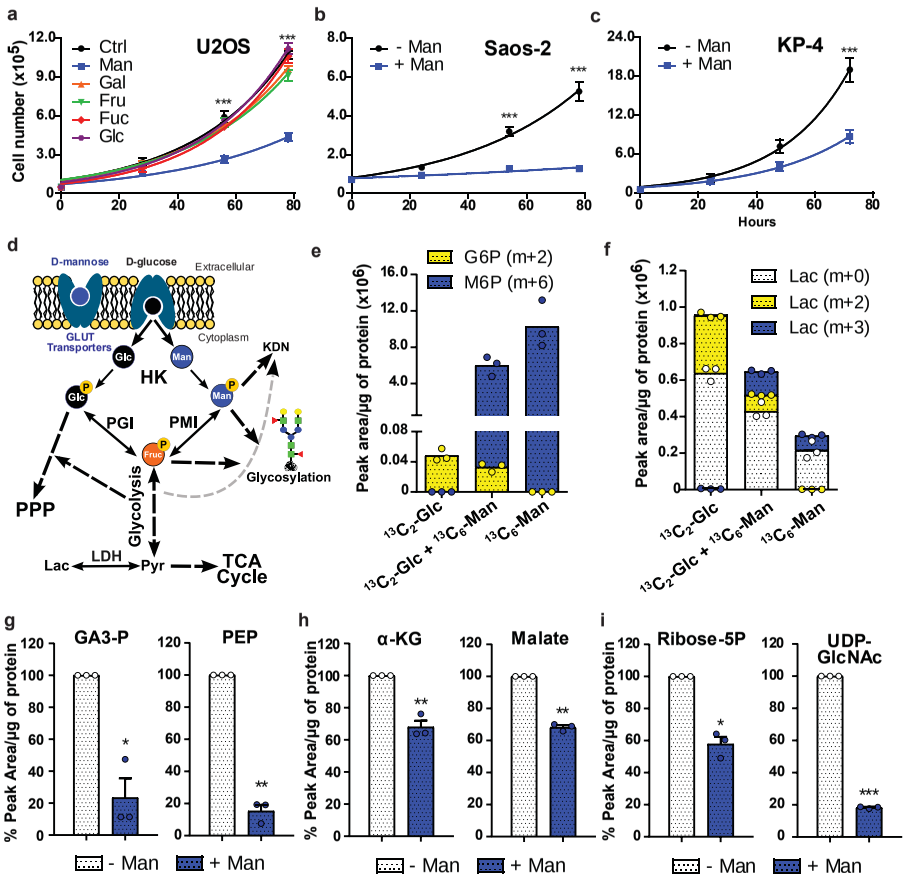
a
U2OS
Ctrl
Man
Gal
Fru
Fuc
Glc
Cell number (x10^5)
b
Saos-2
- Man
+ Man
c
KP-4
Hours
d
D-mannose
D-glucose
Extracellular
GLUT Transporters
Cytoplasm
HK
KDN
PGI
PMI
Glycosylation
PPP
Glycolysis
LDH
Lac
Pyr
TCA Cycle
e
G6P (m+2)
M6P (m+6)
Peak area/µg of protein (x10^6)
f
Lac (m+0)
Lac (m+2)
Lac (m+3)
g
GA3-P
PEP
% Peak Area/µg of protein
h
α-KG
Malate
i
Ribose-5P
UDP-GlcNAc

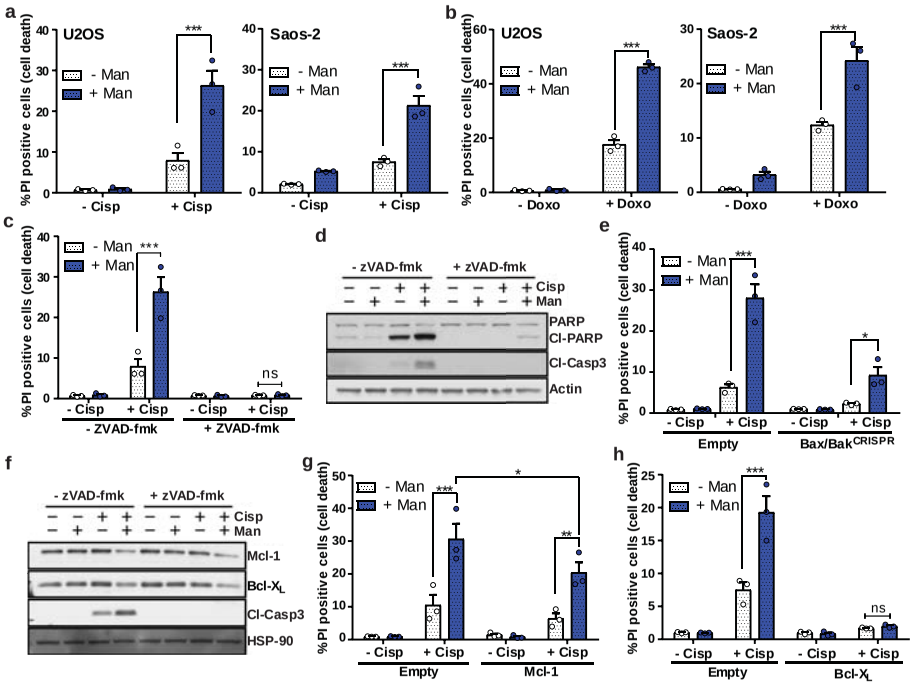
a
U2OS
Saos-2
- Man
+ Man
%PI positive cells (cell death)
- Cisp
+ Cisp
***
b
U2OS
Saos-2
- Doxo
+ Doxo
c
- ZVAD-fmk
+ ZVAD-fmk
ns
d
- zVAD-fmk
+ zVAD-fmk
Cisp
Man
PARP
Cl-PARP
Cl-Casp3
Actin
e
Empty
Bax/Bak CRISPR
*
f
Mcl-1
Bcl-XL
Cl-Casp3
HSP-90
g
Mcl-1
**
h
Bcl-XL

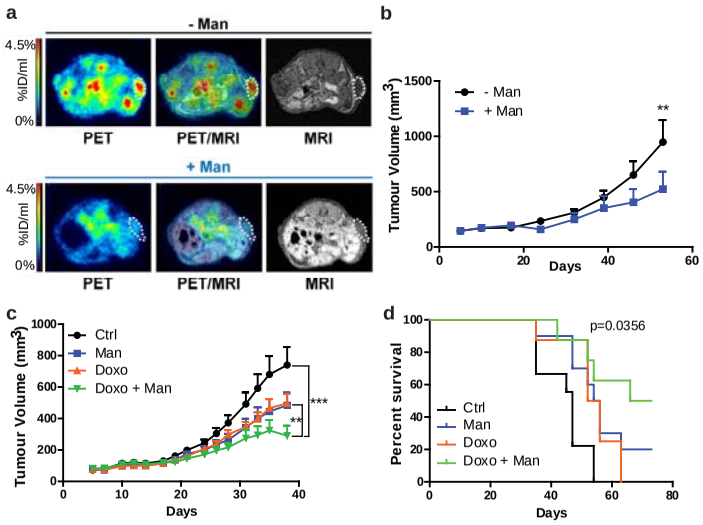
a
- Man
4.5%
%ID/ml
0%
PET
PET/MRI
MRI
+ Man
4.5%
%ID/ml
0%
PET
PET/MRI
MRI
b
Tumour Volume (mm3)
- Man
+ Man
**
Days
c
Tumour Volume (mm3)
Ctrl
Man
Doxo
Doxo + Man
***
**
Days
d
Percent survival
p=0.0356
Ctrl
Man
Doxo
Doxo + Man
Days

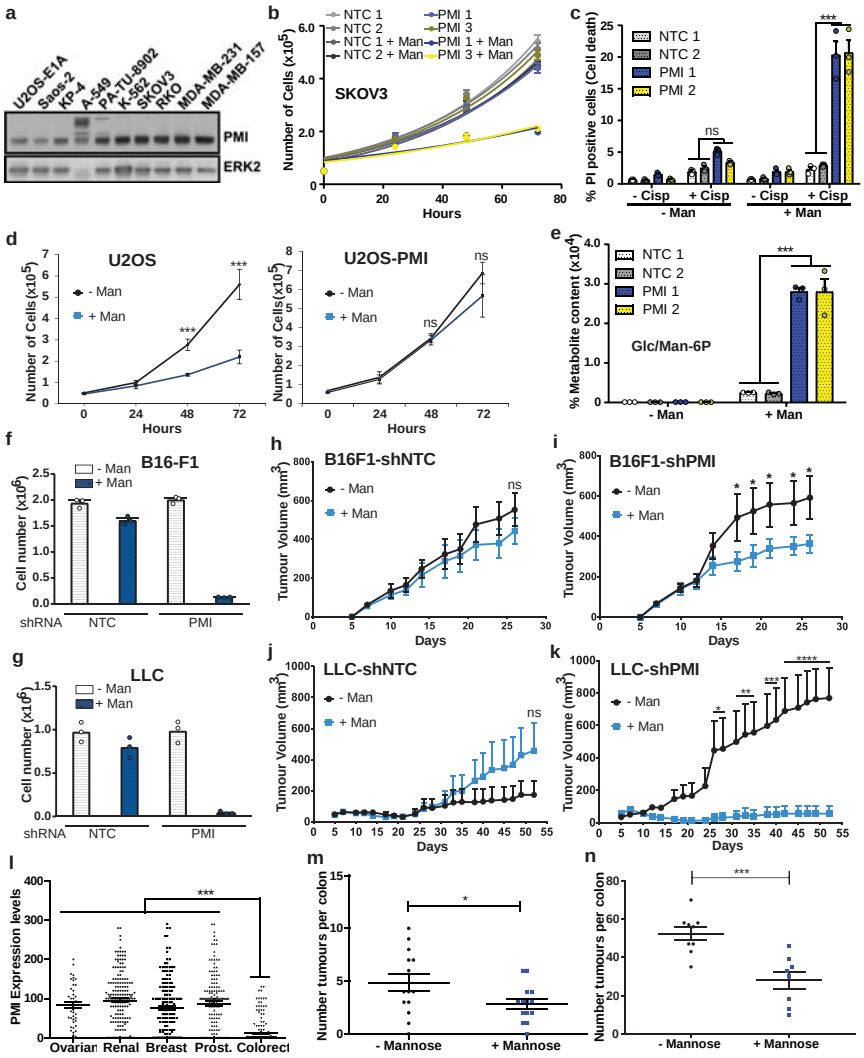
a
U2OS-E1A
Saos-2
KP-4
A-549
PA-TU-8902
K-562
SKOV3
RKO
MDA-MB-231
MDA-MB-157
PMI
ERK2
b
NTC 1
NTC 2
NTC 1 + Man
NTC 2 + Man
PMI 1
PMI 3
PMI 1 + Man
PMI 3 + Man
SKOV3
Number of Cells (x10^5)
Hours
c
NTC 1
NTC 2
PMI 1
PMI 2
% PI positive cells (Cell death)
ns
***
- Cisp
+ Cisp
- Man
+ Man
d
U2OS
U2OS-PMI
- Man
+ Man
Number of Cells (x10^5)
Hours
***
ns
e
NTC 1
NTC 2
PMI 1
PMI 2
Glc/Man-6P
% Metabolite content (x10^4)
f
B16-F1
- Man
+ Man
Cell number (x10^6)
shRNA
NTC
PMI
g
LLC
h
B16F1-shNTC
Tumour Volume (mm^3)
Days
i
B16F1-shPMI
j
LLC-shNTC
k
LLC-shPMI
l
PMI Expression levels
Ovarian
Renal
Breast
Prost.
Colorect
m
Number tumours per colon
- Mannose
+ Mannose
n

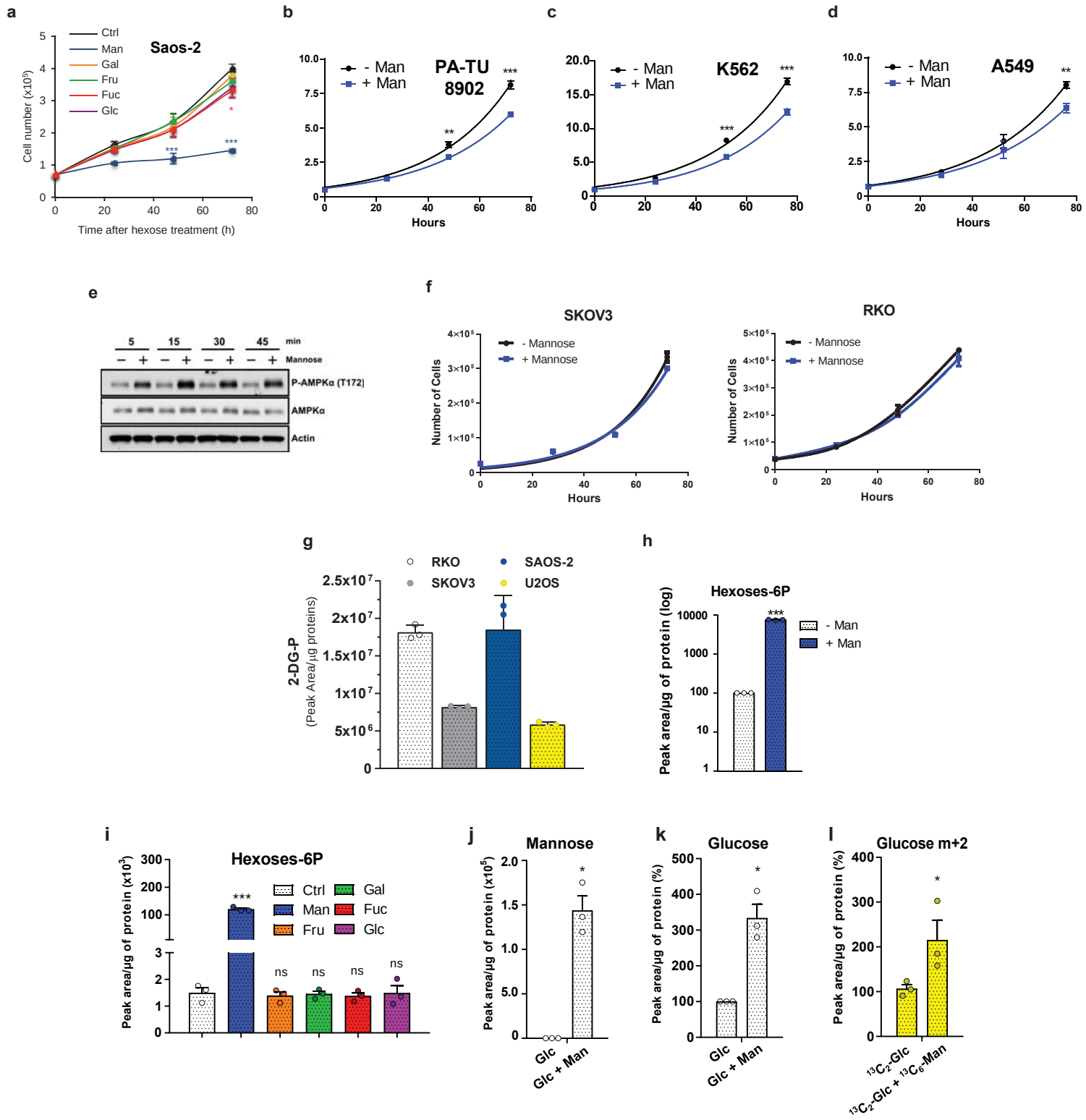

Sierra Gonzalez et al. Extended Data Figure 1

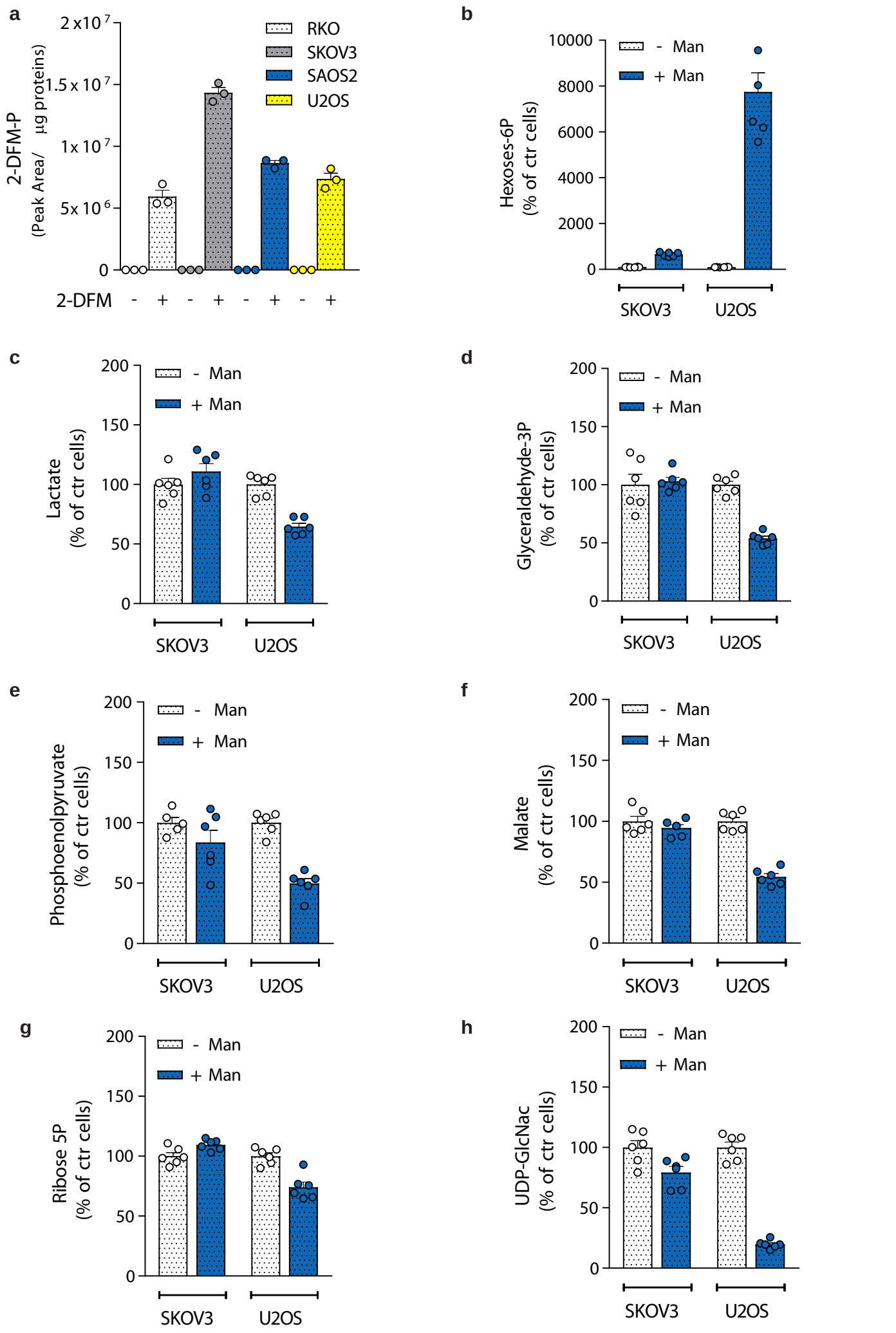

Sierra Gonzalez et al. Extended Data Figure 2

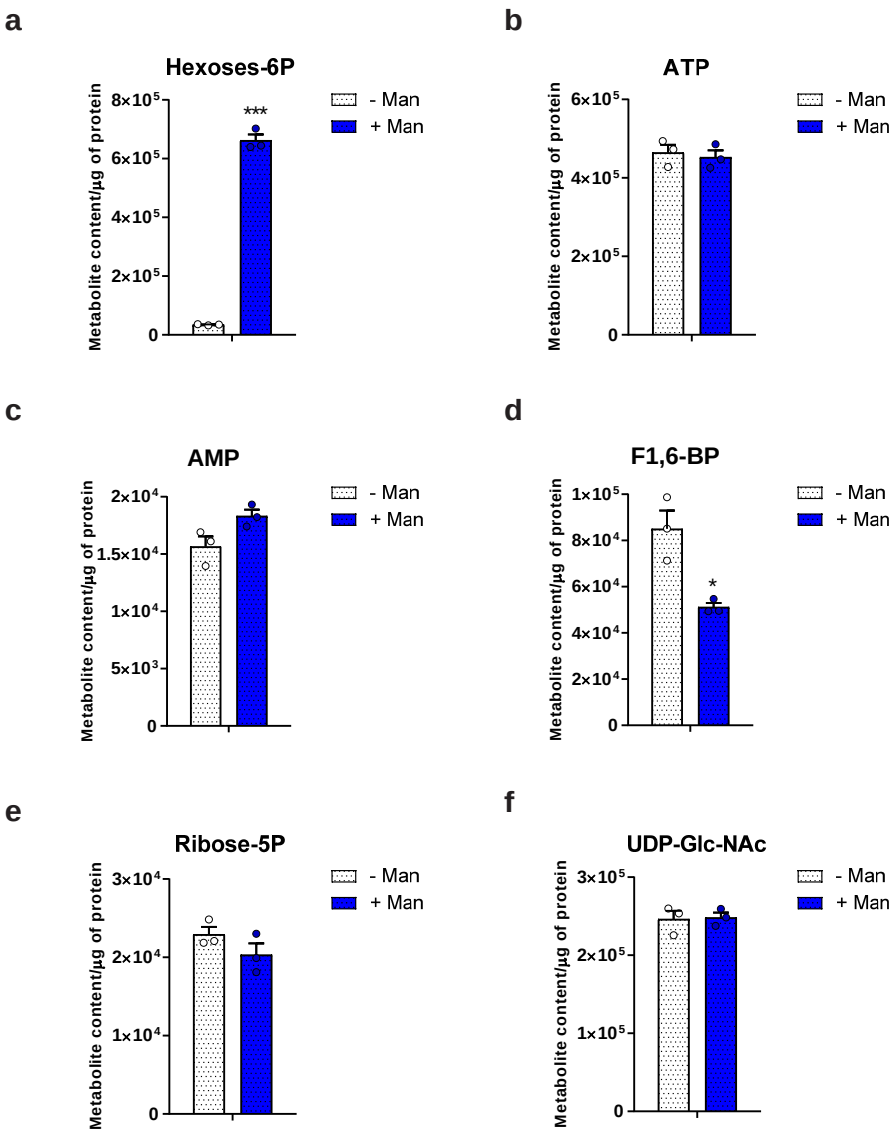

Sierra Gonzalez et al. Extended Data Figure 3

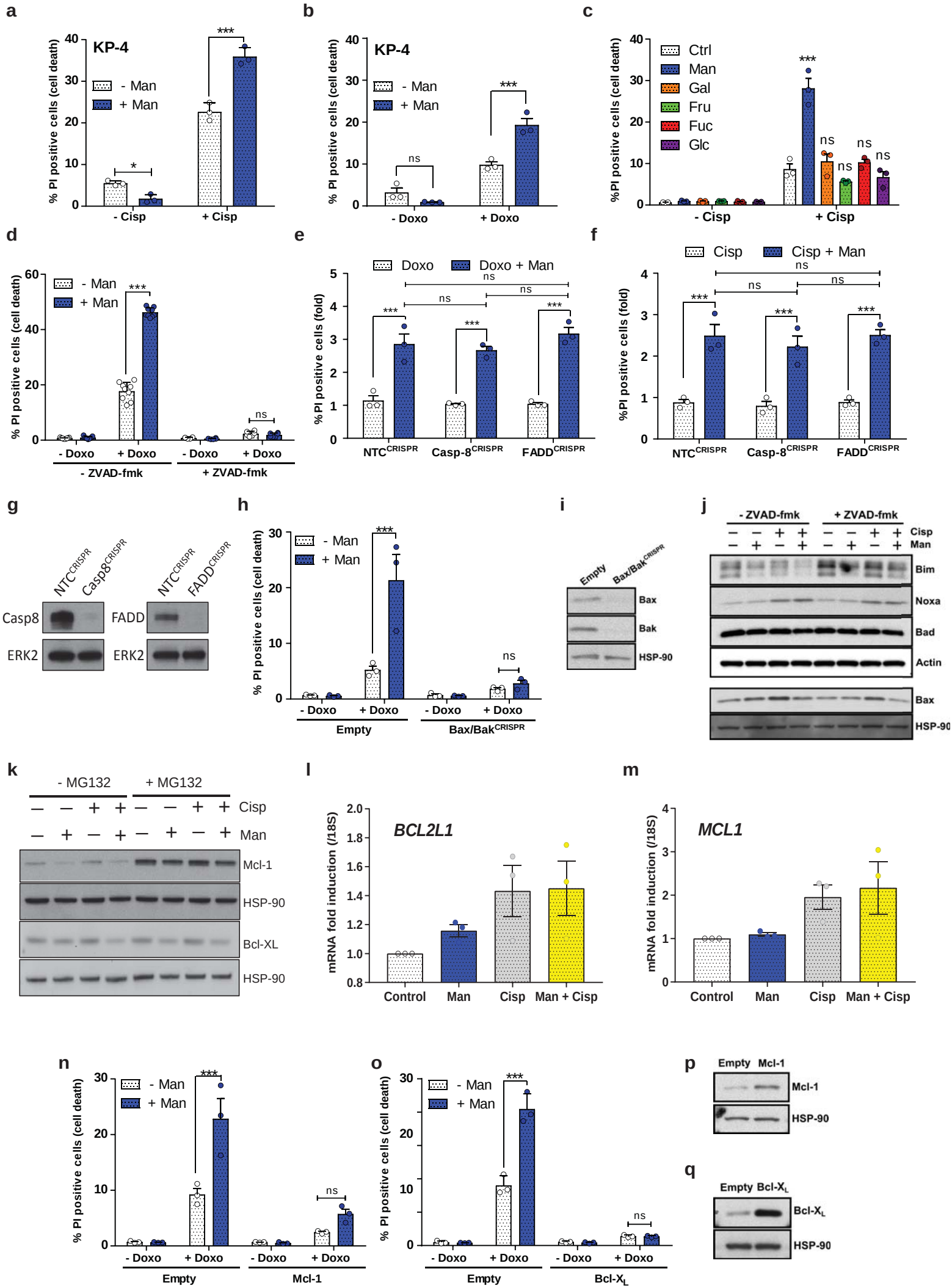

Sierra Gonzalez et al. Extended Data Figure 4

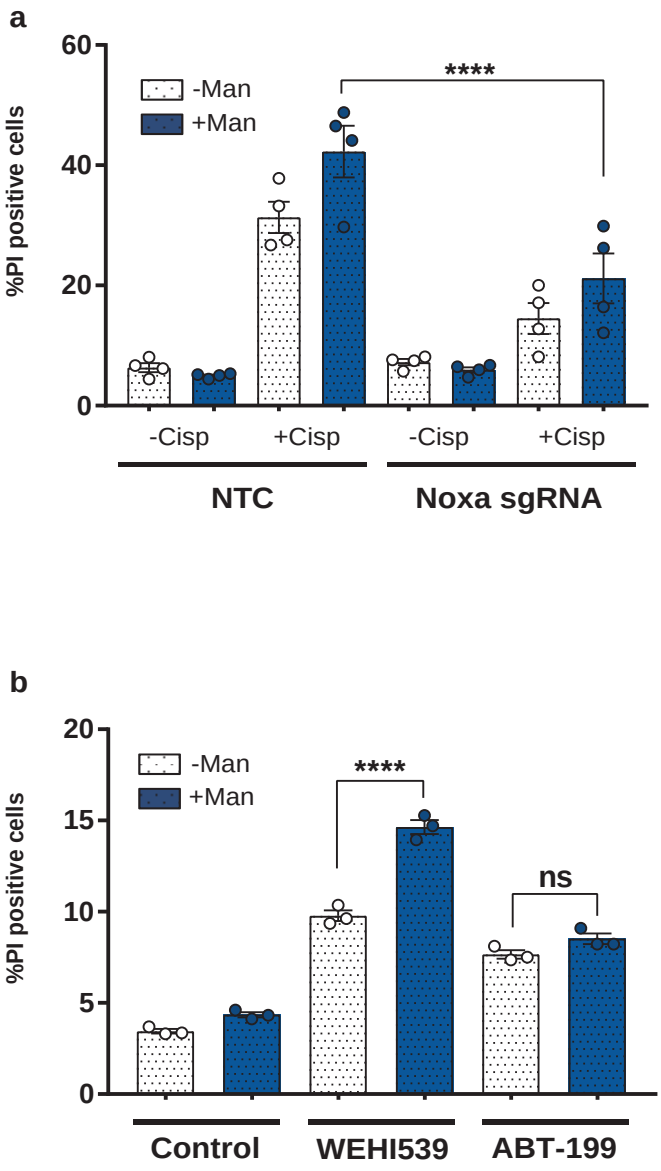

Sierra Gonzalez et al. Extended Data Figure 5

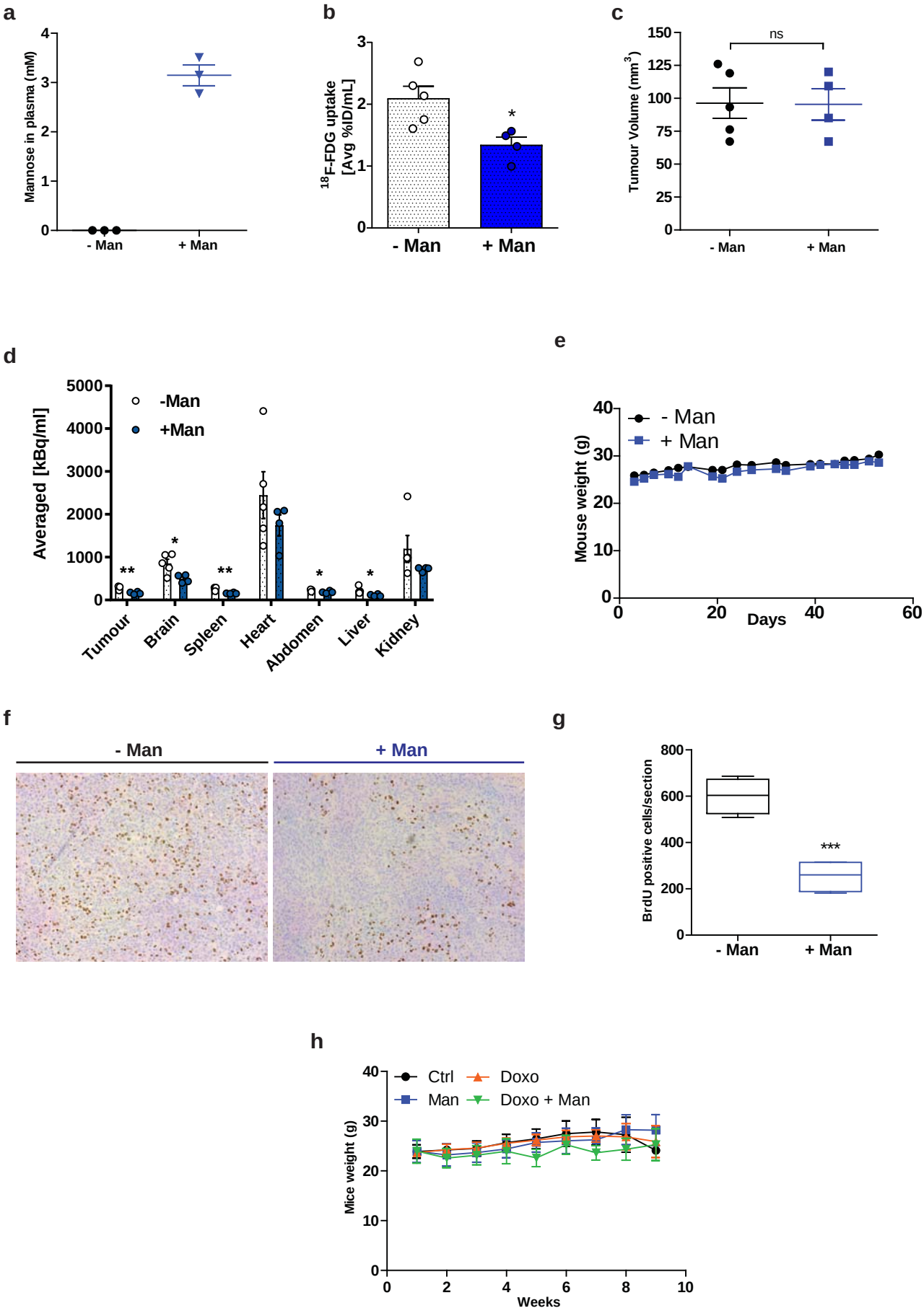

Sierra Gonzalez et al. Extended Data Figure 6

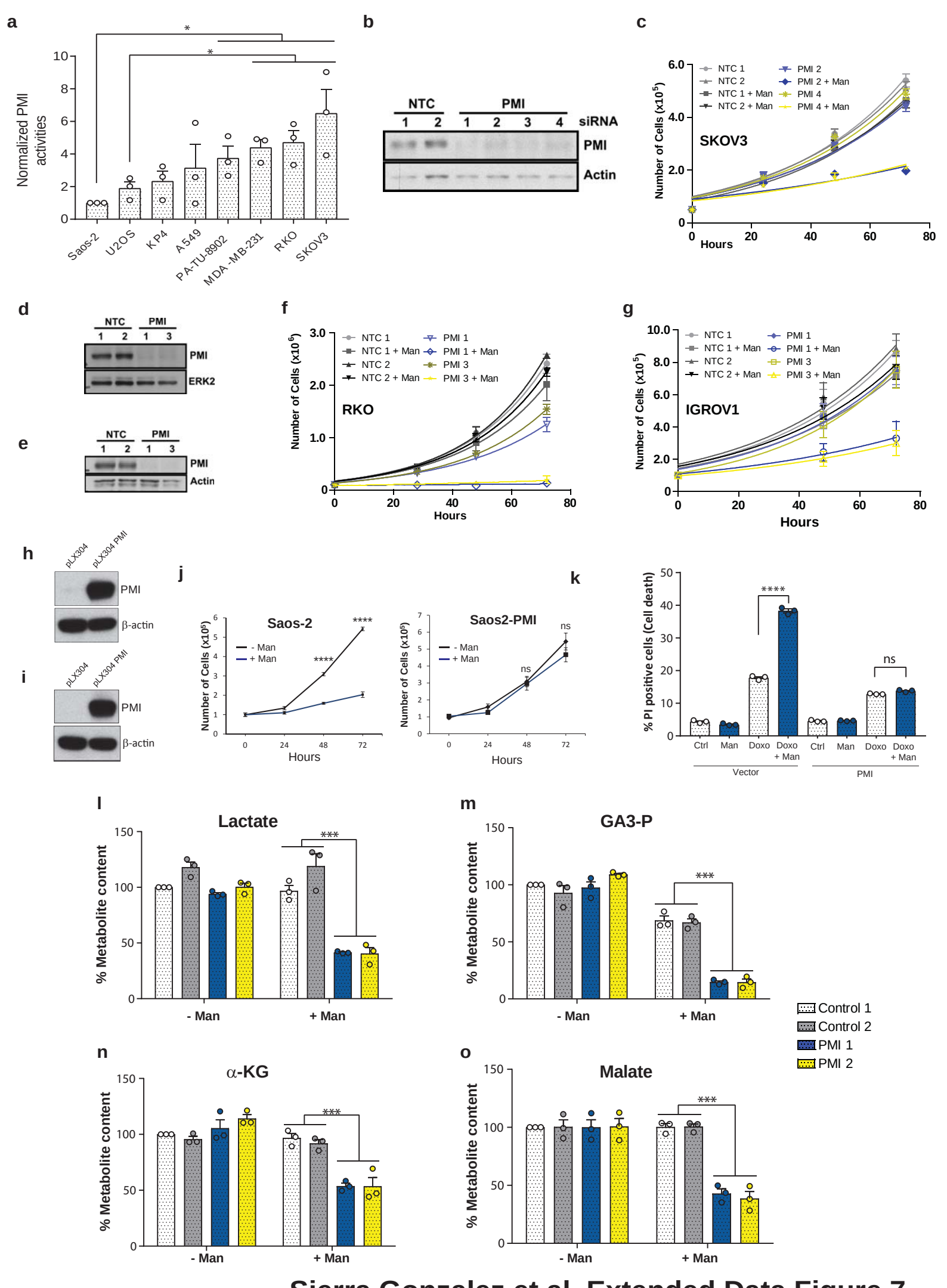

Sierra Gonzalez et al. Extended Data Figure 7

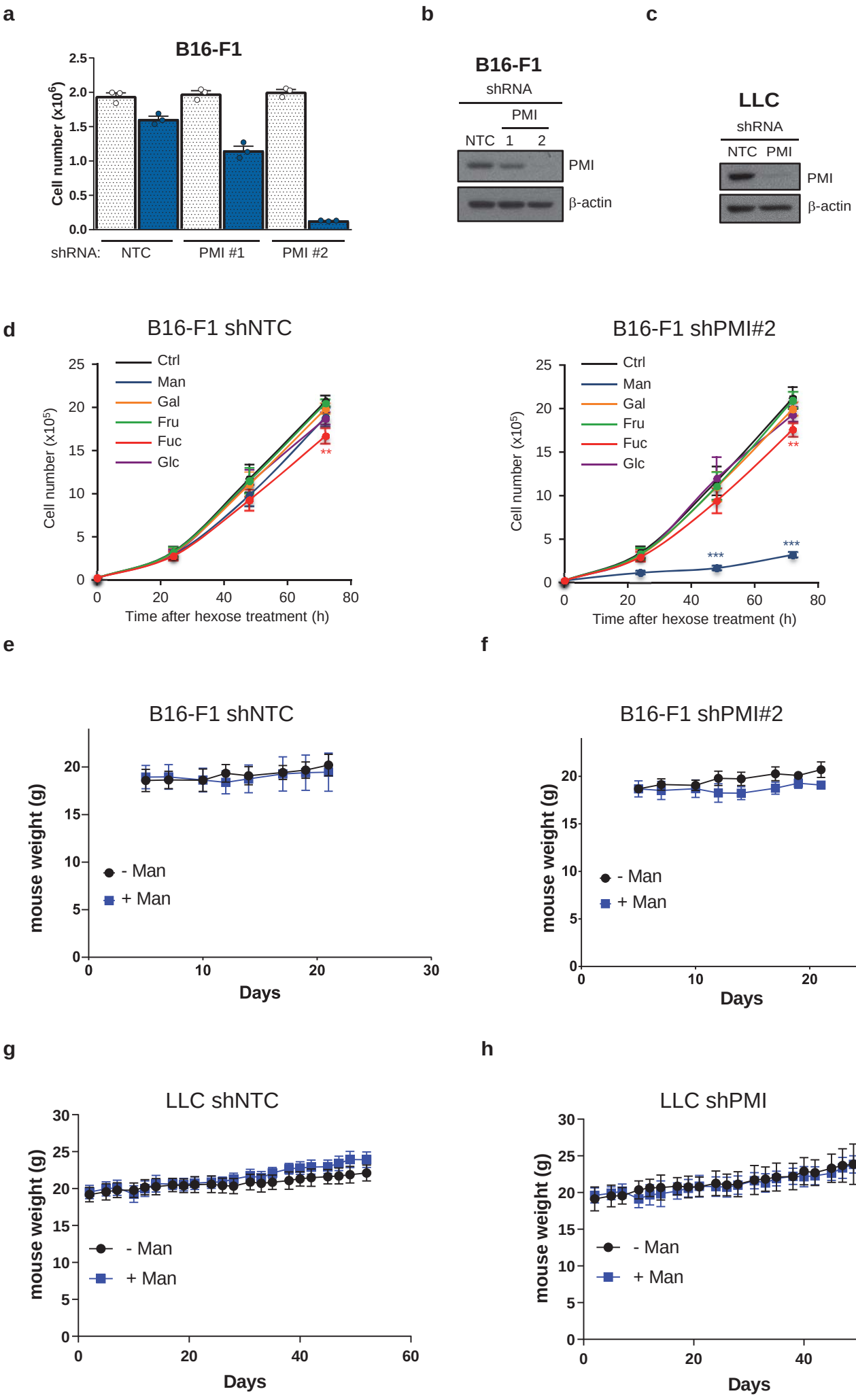
a
B16-F1
Cell number (x10^6)
2.5
2.0
1.5
1.0
0.5
0.0
shRNA: NTC PMI #1 PMI #2
b
B16-F1
shRNA
PMI
NTC 1 2
PMI
β-actin
c
LLC
shRNA
NTC PMI
PMI
β-actin
d
B16-F1 shNTC
Ctrl
Man
Gal
Fru
Fuc
Glc
Cell number (x10^5)
Time after hexose treatment (h)
**
B16-F1 shPMI#2
***
e
B16-F1 shNTC
mouse weight (g)
- Man
+ Man
Days
f
B16-F1 shPMI#2
g
LLC shNTC
h
LLC shPMI

a

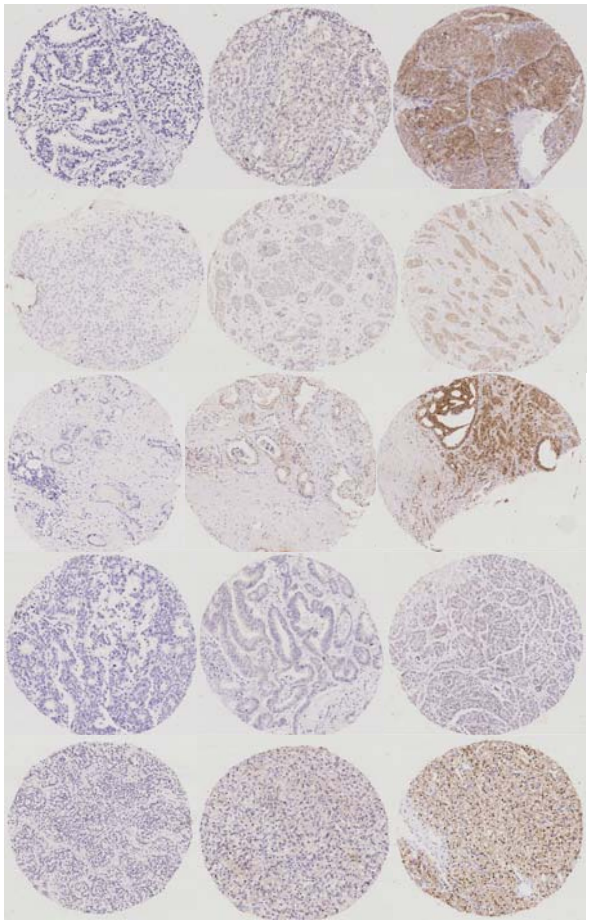

b

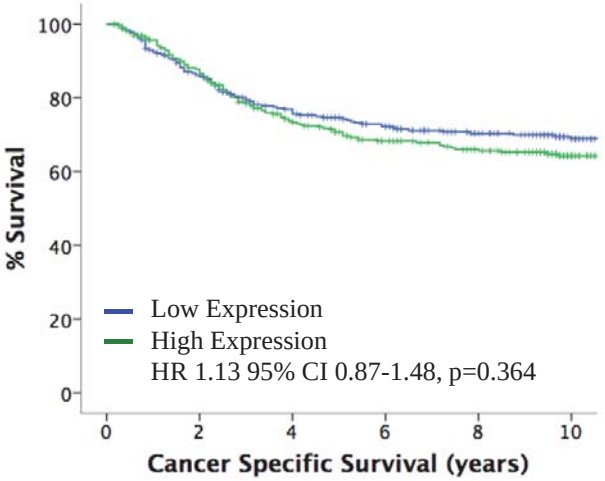

c

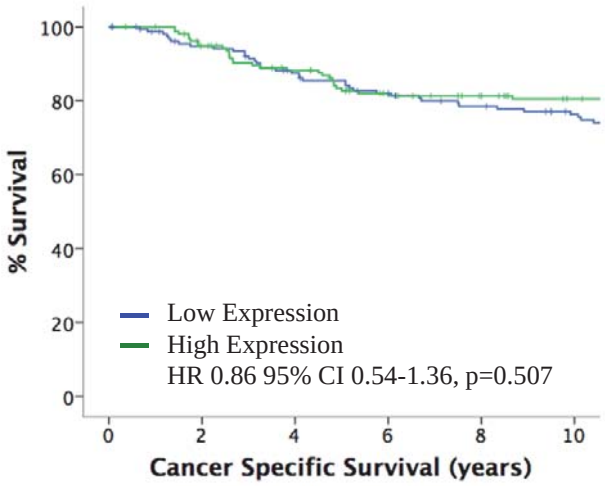

d

	Colorectal Cancer (n=698)			Breast Cancer (n=316)		
	N (%)	10yr CSS (SE)	*P*	*N (%)*	10yr CSS (SE)	*P*
Cytoplasmic PMI (n=698)			0.364			0.507
Low expression	347 (50)	69 (3)		157 (50)	76 (4)	
High expression	351 (50)	64 (3)		159 (50)	81 (3)	

e

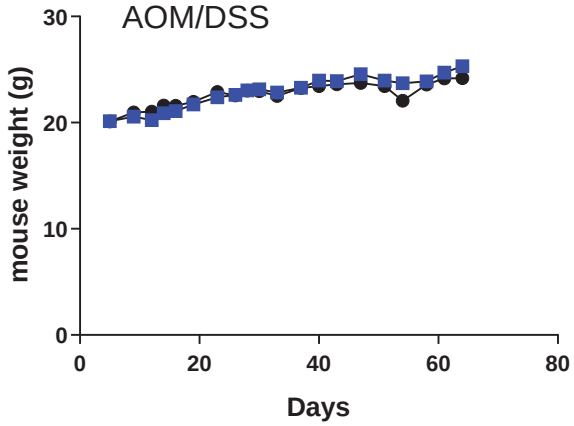

f

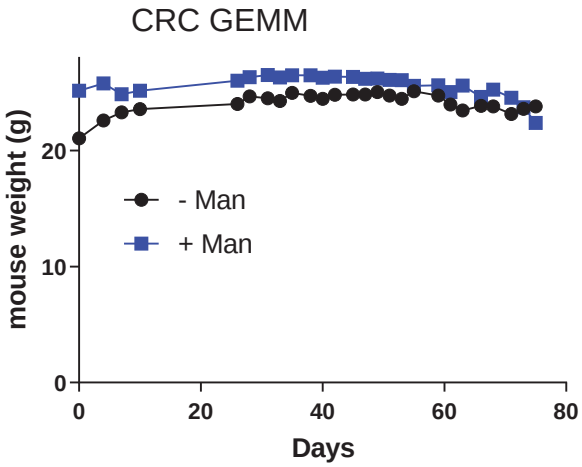

Sierra Gonzalez et al. Extended Data Figure 9

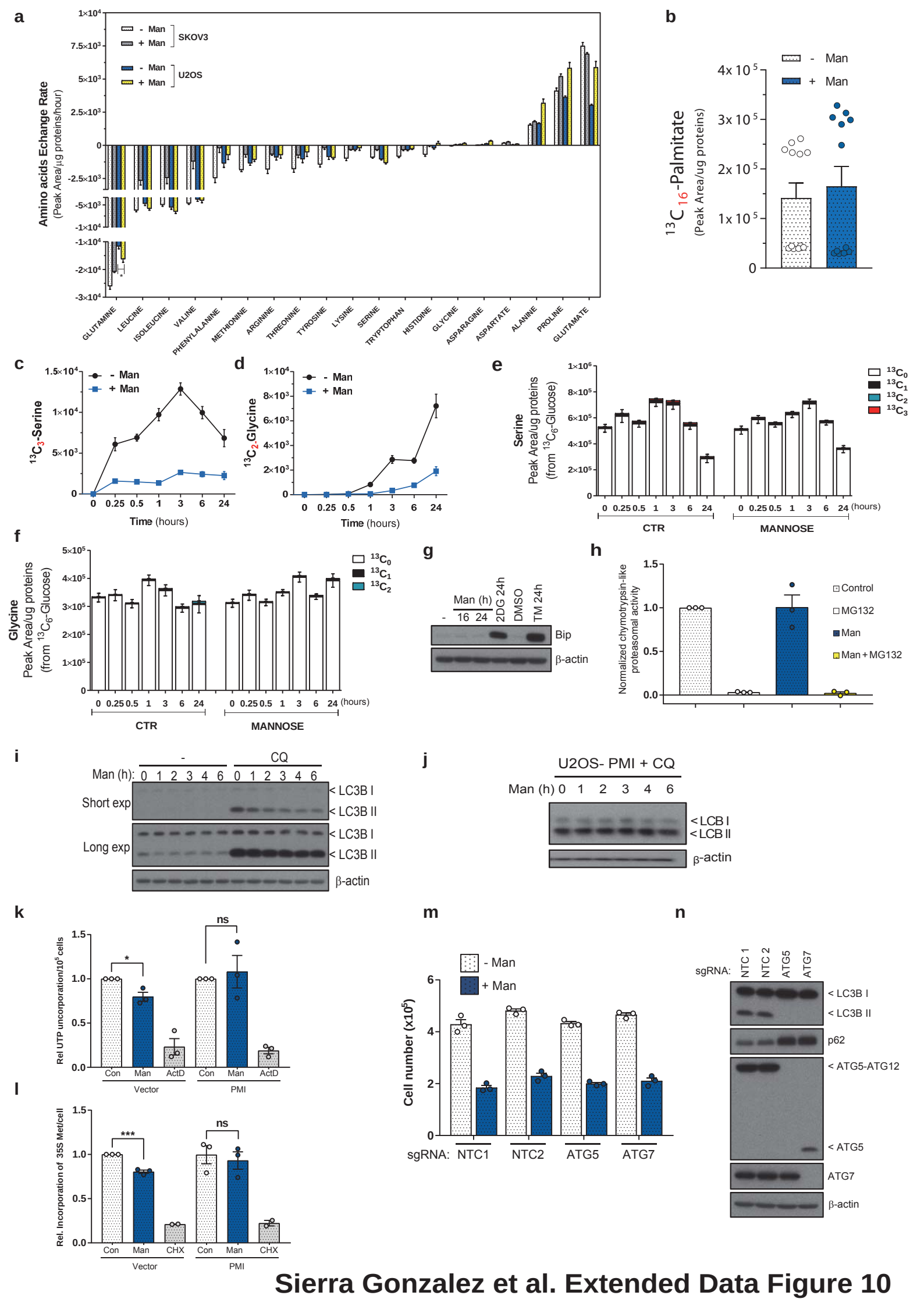

Sierra Gonzalez et al. Extended Data Figure 10